NASA CR–132604

RESEARCH REPORT

ACOUSTICAL CHARACTERISTICS OF THE NASA – LANGLEY FULL-SCALE WIND TUNNEL TEST SECTION

By
A. L. Abrahamson
P. K. Kasper
R. S. Pappa

Prepared for:

NATIONAL AERONAUTICS AND SPACE ADMINISTRATION
LANGLEY RESEARCH CENTER
HAMPTON, VIRGINIA 23665

CONTRACT NUMBER NAS1–12841

WYLE LABORATORIES REPORT NUMBER WRH–74–2

March 1975

WYLE LABORATORIES
SCIENTIFIC SERVICES & SYSTEMS GROUP
3200 MAGRUDER BLVD., HAMPTON, VIRGINIA

ABSTRACT

The full-scale wind tunnel at NASA-Langley Research Center was designed for low-speed aerodynamic testing of aircraft. Sound absorbing treatment has been added to the ceiling and walls of the tunnel test section to create a more anechoic condition for taking acoustical measurements during aerodynamic tests. This report provides the results of an experimental investigation of the present acoustical characteristics of the tunnel test section. The experimental program included measurements of ambient noise levels existing during various tunnel operating conditions, investigation of the sound field produced by an omnidirectional source, and determination of sound field decay rates for impulsive noise excitation. A comparison of the current results with previous measurements has shown that the added sound treatment has improved the acoustical condition of the tunnel test section. An analysis of the data indicated, however, that sound reflections from the tunnel ground-board platform could create difficulties in the interpretation of actual test results. Although not available for this test series a sound-absorbing ground-board platform has since been fabricated and is expected to minimize this problem.

TABLE OF CONTENTS

LIST OF TABLES

LIST OF FIGURES

LIST OF FIGURES (continued)

LIST OF FIGURES (continued)

ACOUSTICAL CHARACTERISTICS OF THE NASA-LANGLEY FULL-SCALE WIND TUNNEL TEST SECTION

1.0 INTRODUCTION

With the emergence of acoustic noise profiles during takeoff and landing as important aircraft design criteria, wind tunnels, originally intended for aerodynamic testing, have been required to perform a new category of functions in aeroacoustic research and development (Reference 1). Since most existing wind tunnel facilities were designed for the purpose of studying aerodynamic properties and not for measurements of aeroacoustic fields, they usually require modification before meaningful acoustic tests may be performed.

The investigation described in this report was the third of a series aimed at defining and improving the acoustic environment of the NASA-Langley full-scale wind tunnel prior to conducting aeroacoustic tests.

The first study (Reference 2) consisted of an experimental investigation of the acoustic characteristics of the full-scale wind tunnel. The results provided evidence of the acoustic characteristics of the test section, and provided a quantitative assessment of the distance from an omnidirectional noise source within which acoustic measurements could be taken. It was indicated that this range could be increased through judicious placement of sound-absorbing material.

The second study (Reference 3) led from this conclusion to investigate, by means of an acoustic model, the most cost-effective placement of sound-absorbing material. Based on recommendations contained in this study, sound-absorbing material was installed on the roof of the test section, and on the east and west walls of the test section above test platform height.

2.0 OUTLINE OF THE CURRENT STUDY

The current study followed naturally on the earlier work and arose out of the need to:

a. Assess the effect of the sound-absorbent material on the reflected acoustic field in the test section,

b. Formulate guidelines for future acoustic measurements in the test section.

The experimental results obtained in this study provided evidence of the non-diffuse acoustic environment in the test section. In addition, comparison with a theoretical model indicated a predominant source of local reflection apparently from the test platform. The acoustic treatment for the platform recommended in Reference 3, was still in the process of fabrication and consequently had not been installed for the current tests. In view of this, it is suggested that the tests be repeated at a later date.

3.0 TEST PROCEDURE AND ANALYSIS OF RESULTS

The test procedure was designed with the above objectives, and consisted of three types of acoustic measurements:

a. Ambient noise in various modes of tunnel operation,

b. Sound field of an omnidirectional source,

c. Decay rate for impulsive sounds.

This procedure was similar to that followed in the first study (Reference 2) to facilitate comparison with the results obtained prior to installation of the sound-absorbent material (Reference 3).

3.1 Ambient Noise Level

Sketches of the top and side views of the test section of the full-scale wind tunnel appear in Figure 1. Octave-band ambient noise levels with no airflow in the tunnel were measured at each of the four microphone positions indicated in the figure. An intermittant noise source was identified as a compressor in the south end of the building. The ambient levels at microphone position 4 were measured both with and without this compressor operating. For subsequent tests the compressor was switched off. Figure 2 displays octave-band frequency analyses of these four sets of ambient noise measurements. For all microphone positions, the octave-band levels with the compressor turned off fell approximately within a 5-dB spread.

With the tunnel running, the ambient level increased in all octave bands with increasing airspeed. The family of curves generated by measurements at five tunnel speeds is shown in Figure 3a, 3b, and 3c for microphones at positions 2, 3, and 4 respectively. Examination of the curves reveals a sound pressure level increase in each octave band of approximately 18 dB for a doubling of airspeed.

Following the procedure proposed in Reference 2 to demonstrate the sixth power dependence on velocity more clearly, the ambient octave-band levels were normalized by subtracting $60 \log_{10} u$ (where u is the airspeed in mph) from each value. The ranges of normalized octave-band levels for each microphone position, calculated from the data at 6 airspeeds presented in Figures 3a through 3c, are shown in Figure 4. The data spread of normalized levels for each position is small and virtually constant at 3 dB for all nine octave bands. Since the spreads are so small, it is reasonable to estimate the octave-band levels at other airspeeds than those chosen for the test by adding $60 \log_{10} u$ to the normalized levels of Figure 4.

To compare the normalized ambient levels in the test section before and after installation of the sound absorbent material, the mean of these normalized noise levels measured at positions 2, 3, and 4 was calculated for each octave band. These mean levels are compared in Figure 5 with similarly obtained normalized levels reported in Reference 2 from measurements at three comparable microphone positions.

It may seem that addition of the sound-absorbent material has resulted in a lower ambient noise level in the test section over all airspeeds. This is shown as a decrease in the normalized level of approximately 2 dB at 31.5 Hz rising to a 7-dB drop at 8 kHz.

A narrow-band frequency analysis was conducted for the recorded acoustic data at several tunnel speeds. Examples presented in Figure 6 show that large sharp peaks are present in the spectrum below about 100 Hz. From their shift along the frequency scale, which is proportional to tunnel speed, these are evidently propellor rotational-noise components.

Care should therefore be applied when evaluating results of any future acoustic tests in the full-scale tunnel at frequencies below 100 Hz. Similar narrow-band analyses in specific cases would assist in separating spectral peaks due to tunnel propellors from those due to test aircraft noise.

3.2 The Sound Field of an Omnidirectional Noise Source Located Above the Center of Test Platform

3.2.1 Background

In general, the acoustic field established by a sound source within a room is composed of the direct sound from the source and the multiply-reflected or reverberant sound. The intensity of the direct sound decreases with increasing distance from the source while, in general, the spatial distribution of the reverberant sound is a function not only of the geometry and sound-absorbing properties of all interior room surfaces, but also of the directional and spectral characteristics of the source. For simplified analytical purposes, it is often assumed that the reverberant sound level is constant throughout the room. The validity of this assumption is approached by "well-behaved" semireverberant rooms having nearly uniform spatial distribution of sound-absorbing surfaces.

The sound pressure level of the direct sound from a nondistributed source can be expressed as (Reference 4):

$$SPL_d = PWL + 10 \log_{10}\left(\frac{Q(\theta,\psi)}{r^2}\right) - 0.5 \text{ dB} \qquad \text{(Eq. 1)}$$

where

SPL_d = direct sound pressure level (dB re 20×10^{-6} N/m^2)

PWL = acoustic source strength (dB re 10^{-12} watt)

$Q(\theta, \psi)$ = directivity factor of source (dimensionless)

θ, ψ = azimuth and elevation of measurement position

r = distance to acoustic center of source (ft)

Thus, the direct sound pressure level will decrease by 6 dB for each doubling of the measurement distance from the source in any radial direction, independent of the source strength and its directivity.

If the acoustic energy of the reverberant field is uniformly distributed throughout the entire room, the field is said to be diffuse. Under such ideal conditions, the reverberant sound level in a room is only a function of the acoustic power

output of the sound source and of the total room absorption, and is given by (Reference 4):

$$SPL_r = PWL - 10 \log_{10} a + 16.5 \qquad \text{(Eq. 2)}$$

where SPL_r = reverberant sound pressure level (dB re 20×10^{-6} N/m^2)

PWL = acoustic source strength (dB re 10^{-12} watt)

a = total room absorption (sabins)

The total sound pressure level at a distance r from a source is the decibel sum of the direct sound level (Equation 1) and the reverberant sound level (Equation 2). Its value is:

$$SPL = PWL + 10 \log_{10}\left(\frac{Q(\theta, \psi)}{4\pi r^2} + \frac{4}{a}\right) + 10.5 \qquad \text{(Eq. 3)}$$

for SPL in dB re 20×10^{-6} N/m^2

PWL, dB re 10^{-12} watt

r, ft

a, sabins

For an omnidirectional source, Q = 1 for all θ and ψ. The difference SPL - PWL from Equation 3, for Q = 1, is plotted in Figure 7 as a function of the total room absorption, a.

At some radial distance from the source, say r*, the direct sound level will equal the reverberant sound level. This distance, which can be considered as the transition point between the direct and the reverberant sound fields, has been termed the "hall radius", by several recent investigators (e.g., Reference 2). Its value, obtained by equating the two terms in parentheses of Equation 3, is given by:

$$r^* = 0.141\, a^{1/2} \qquad \text{(Eq. 4)}$$

where a = total room absorption

The hall radius, r*, may also be determined graphically from Figure 7. Note that each curve asymptotically approaches a specific reverberant sound level for a specified amount of total absorption. If the total absorption in the room is known, the intersection of the corresponding reverberant level horizontal asymptote and the -6 dB/doubling of distance line of the direct sound field will locate the value for r*. Because the direct and reverberant sound fields are equal in intensity at this intersection point, the total sound pressure level at the hall radius distance will be 3 dB greater than that expected at the same radial distance in the absence of reflections.

3.2.2 Measurements Before Addition of Sound Absorbing Material

The measurement and analysis in this section were reported in Reference 2, and represent a simplified description for the sound field in the test section of the NASA-Langley full-scale wind tunnel. The sound field of a broadband "omnidirectional" source suspended above the center of the test platform was measured in the vertical, and in horizontal directions perpendicular to the walls of the test section. Octave-band sound pressure levels for each direction were plotted as a function of distance from the source. The magnitude of the sound field was found practically independent of direction for all octave bands. A mean "hall radius" was then calculated for each octave band from best-fit lines through data points (Figure 11).

3.2.3 Measurements After Addition of Sound Absorbing Material

The acoustics of large absorbent rooms are not generally representable by the simple assumptions made in deriving Equation 3 of section 3.2.1. The classical "Sabine Assumption" of a diffuse reverberant field is particularly inapplicable when the room absorption is large and concentrated in localized areas. In this case, the reverberant sound field, rather than being diffuse, is dominated by first and second reflections. These result in phase reinforcement and cancellation and give rise to the presence of spatial maxima and minima in the established sound field.

In contrast to the earlier experiment, the current set of measurements of the sound field about an omnidirectional source disclosed strong directional non-

uniformities. Measurements were made using a pink noise spectrum as input to the source which was located relative to the test platform and measurement positions shown in Figure 8.

To examine the nonuniform decay of the sound field with distance, irregularities in the radiation pattern of the source were removed by relating measurements in a particular direction to measurements made in the same direction at a distance of 5 feet from the source. These values of relative sound pressure level are presented in Figures 9a through 9h for octave-band center frequencies 63 Hz through 8 kHz, respectively. For reference, the theoretical free-field decrease of 6 dB per doubling of distance is superimposed through the 5-foot data point in each plot.

Since measurements in the west direction extended farther than in other directions, these were chosen for closer examination. For convenience, they are grouped together in Figure 10, where it may be seen that several maxima and minima occur where a smooth exponential decay with distance might be expected.

To attempt an analytical explanation of these perturbations, a mathematical model was constructed and translated into a computer program. The basic assumption made in this model was that all reflected sound could be ignored except that from the test platform. This assumption is justified for a first-order model due to the relative proximity of the platform to the source compared with other reflecting surfaces, and also due to the high reflection coefficient of the test platform compared to other reflecting surfaces. Since no absorbent material was installed on the platform during the current tests, it was assumed that the platform was a perfect reflecting surface.

Each octave band of noise was decomposed into a large number of sinusoidal components whose magnitudes were weighted by a pink noise spectral distribution, which were then added vectorially at each frequency component for the direct and reflected waves. The resultant sums were combined to form an interference field in the westerly direction for each octave band as shown in Figure 10. (Similar work is reported in References 5 and 6). The sharp drop at a horizontal distance of 42 feet is representative of the sudden absence of the reflected wave as the platform ends. Comparisons in Figure 10, of the measured sound field and that calculated from the first-order reflection model described above, show similar trends. This similarity, combined with the relative proximity of the test platform and the source compared with other reflecting surfaces, is considered sufficient to conclude that reflections from

the test platform are a major contributing factor to the deviation from exponential decay of sound pressure level with distance from the source

Clearly, a complete explanation of all observed phenomena in the sound field requires a substantially more complex model incorporating additional first and higher-order reflections, adjustments for source directivity, and substitution of actual impedances at reflecting surfaces. For example, if the phase change on reflection at the platform were -90° at 125 Hz due to structural resonance, there would be improved agreement with measured data as shown in Figure 10.

A direct comparison of measured data with that from the previous experiment from Reference 2 is shown in Figure 9e. Only the 1000-Hz octave-band data from Reference 2 was available for the comparison; however, the figure shows that levels of reflected sound are generally lower than in the previous experiment.

Due to the nonuniform decay of SPL with distance, combined with directional dependence, it was not possible to derive hall radius values in the same manner as in Reference 2. Instead, a parameter analogous to the hall radius, but purely empirical in character, was used. This parameter is measured under the assumption that near the source only the direct field is significant. The direct field at larger distances is then calculated from an inverse square law decay (6 dB for doubling of distance) superimposed on a measurement of sound pressure level taken near the source.

The distance at which measured values deviate from the inverse square law decay by 3 dB is taken to be the "modified hall radius". At this point, the reflected sound field equals the direct sound field in power. Values of the modified hall radius derived in this manner are presented in Table I. The average modified hall radius over all measurement directions for each octave band is plotted in Figure 11, and is compared with the hall radius data reported in Reference 2.

Drawing any significant conclusions from this comparison is difficult due to the presence of dominant first-order reflections. In this regard, however, it is clear that the full benefit of the sound-absorbent material on the walls and ceiling of the test section is unlikely to be derived unless adequate sound-absorbent material is also added to the test platform.

3.3 Measurement of Reverberation Time in Test Section

To measure the sound decay rate in the test section, the room was impulsively excited by a gun blast at numerous locations. Source positions near the room corners were chosen in order to excite the highest number of normal modes of the room. Microphones were located at various positions throughout the test section, all at least 40 feet away from the source and at least 10 feet from any wall. From tape-recorded decay signals, octave-band decay charts were obtained with a B & K graphic level recorder at a writing speed of 200 mm/sec and a paper speed of 30 mm/sec. Example decay charts are shown in Figure 12.

The decay curves for octave bands centered at 125 Hz, and above, showed distinctive double-slope character. This is a familiar characteristic of sound decay in rooms having one set of walls more absorbent than the others. In this case, the large duct openings in the north and south walls act as highly absorbent surfaces. The initial slope of the decay curve is representative of the maximum energy absorption rate of the room, and thus, is indicative of the total amount of acoustic absorption within the room (Reference 7).

Fourteen sets of source and microphone locations were used for the test. The average "initial" reverberation times for each octave band, calculated from the initial slope of the decay curves, are presented in Table II. The standard deviation for each data group is also shown. The temperature and relative humidity in the room during the tests were 45°F and 55%, respectively.

These results are compared with those obtained before the addition of sound-absorbent material in Figure 13. The figure shows that reverberation times are apparently reduced in the midfrequency range after addition of the sound-absorbent material. A completely unambiguous comparison is not possible, however, since in rooms of this size, air absorption significantly affects reverberation times, and no record of relative humidity or temperature were reported for the previous set of tests.

To clarify this comparison, an attempt was made to analytically evaluate the effect of different combinations of temperature and relative humidity on reverberation times. This effort failed in its intention but provided further important evidence of the inapplicability of "Sabine acoustics" to the test section of the full-scale wind tunnel.

Reverberation time in a large room, under the Sabine assumption of a diffuse

field, is given by (Reference 8):

$$T = \frac{0.049V}{a+4mV}$$

where

T	=	Reverberation time (seconds)
V	=	Volume of room (cu. ft.) ($\approx 7 \times 10^5$ cu. ft. for test section of full-scale tunnel)
a	=	Absorption of interior enclosure surfaces (sabins)
m	=	Air absorption parameter ($ft.^{-1}$)

For the current test, at a temperature of 45°F and 55% relative humidity, "4m" has the values shown in Table III at octave-band center frequencies. Solving for "a" in the above expression, using these values of "4m", and the experimental reverberation times given in Table II, yields somewhat unexpected results. Above 2000 Hz, values of "a" are negative, indicating a net energy increase on reflection. Clearly, the basic premises must be faulty and an analysis based upon the Sabine assumption is unreliable.

At lower frequencies (octave bands centered on 31.5, 63, and 125 Hz) reverberation times measured during the current test are longer than in the previous test. This is perhaps due to a different interpretation of the decay characteristic, since the presence of a double slope at these frequencies is open to question (see, for example, the upper curve of Figure 12).

4.0 CONCLUSIONS

As originally stated in section 2.0, this study had two objectives:

a. To assess the effect of the addition of sound-absorbing material to the test section,

b. To formulate guidelines for future acoustic measurements in the test section.

With regard to the first objective, it is probable that the anechoic character of the test section of the full-scale wind tunnel has increased due to installation of sound-absorbent material on the side walls and ceiling of the test section. This is indicated by a decrease in ambient noise level during tunnel operation and the decreased reverberation times in the midfrequency range, the magnitude of which are unlikely to result from differences in relative humidity between tests.

During projected aeroacoustic tests, however, noise sources will be mounted above the test platform. In tests of this nature, it is likely that reflections from the platform will mask any significant improvement gained by the installation of the sound-absorbent material. It is therefore suggested that the sound-absorbent material recommended in Reference 3 be installed on the platform surface and that qualification tests with an omnidirectional source be repeated.

In the case of the second objective defined above, it is difficult at this stage to formulate definitive experimental guidelines. In Figure 14, it may be seen that a directional source may cause reflected component magnitudes significantly different from those of an omnidirectional source. In this example, noise directed preferentially towards the ceiling may cause a reflected field of comparable magnitude to the direct field at critical points below the noise source. This effect would not be observed in the case of an omnidirectional noise source.

It is suggested, therefore, that further tests be performed with directional sources, as there is sufficient evidence to indicate that the room is nonuniform in its absorbent characteristics.

REFERENCES

1. Bender, J., et al, "Aeroacoustic Research in Wind Tunnels: A Status Report," NASA CR-114575, Pennsylvania State University, February 1973.

2. Ver, I. L., Malme, C. I., and Meyer, E. B., "Acoustical Evaluation of the NASA Langley Full-Scale Wind Tunnel," NASA CR-111868, January 1971.

3. Ver, I. L., "Acoustical Modeling of the Test Section of the NASA Langley Research Center's Full-Scale Wind Tunnel," BBN Report No. 2280, November 1971.

4. Rettinger, M., "Acoustic Design and Noise Control," Chemical Publishing Co., New York, 1973.

5. Franken, P. A., "A Theoretical Analysis of the Field of a Random Noise Source Above an Infinite Plane," National Advisory Committee for Aeronautics, Technical Note 3557, 1955.

6. Howes, W. L., "Ground Reflection of Jet Noise," NASA Lewis Research Center, Technical Report R-35, 1959.

7. Embleton, T. F. W., "Absorption Coefficients of Surfaces Calculated from Decaying Sound Fields," Journal of the Acoustical Society of America, Vol. 50, 1971, p. 801.

8. Beranek, L. L., (editor), "Noise and Vibration Control," McGraw-Hill Book Company, New York, 1971.

TABLE I
"MODIFIED HALL RADIUS" DISTANCES MEASURED
FROM SPL VS. DISTANCE DATA

Direction from Source	Modified Hall Radius, ft for Octave-Band, Hz of —							
	63	125	250	500	1000	2000	4000	8000
North	17	21	>25	22	>25	>25	>25	>25
South	12	20	>25	20	16	>25	>25	>25
East	13	>20	>20	>20	12	14	>20	>20
West	17	22	26	26	28	20	23	24
Vertical	15	22	19	25	>35	>35	31	>35
Average	14.8	>21.0	>23.0	>22.6	>23.2	>23.8	>24.8	>25.8

" > " signifies that measured octave-band sound pressure levels were always less than 3 dB above the theoretical free-field -6 dB/doubling distance line (passing through measured SPL at 5 ft) for all positions less than maximum measurement distance.

TABLE II

"INITIAL" REVERBERATION TIMES

Octave-Band Center Frequency, Hz	Average Reverberation Time*, sec	Standard Deviation*, sec
31.5	2.26	0.53
63	2.37	0.45
125	2.01	0.21
250	1.84	0.32
500	2.04	0.53
1000	2.05	0.40
2000	1.86	0.32
4000	1.35	0.12
8000	0.94	0.09

*14 Source and microphone sets

TABLE III

Parameters in "Sabine Acoustics" Analysis		
Octave-Band Center Frequency	Volume Absorption Coefficient 4m (ft^{-1})	Absorption of Interior Surfaces, a (Sabins)
31.5	3.62×10^{-5}	1.53×10^{4}
63	7.25×10^{-5}	1.44×10^{4}
125	1.565×10^{-4}	1.61×10^{4}
250	2.89×10^{-4}	1.70×10^{4}
500	5.96×10^{-4}	1.18×10^{4}
1000	1.46×10^{-3}	5.70×10^{3}
2000	4.29×10^{-3}	-1.1×10^{4}
4000	1.27×10^{-2}	-6.27×10^{4}
8000	3.64×10^{-2}	-2.12×10^{5}

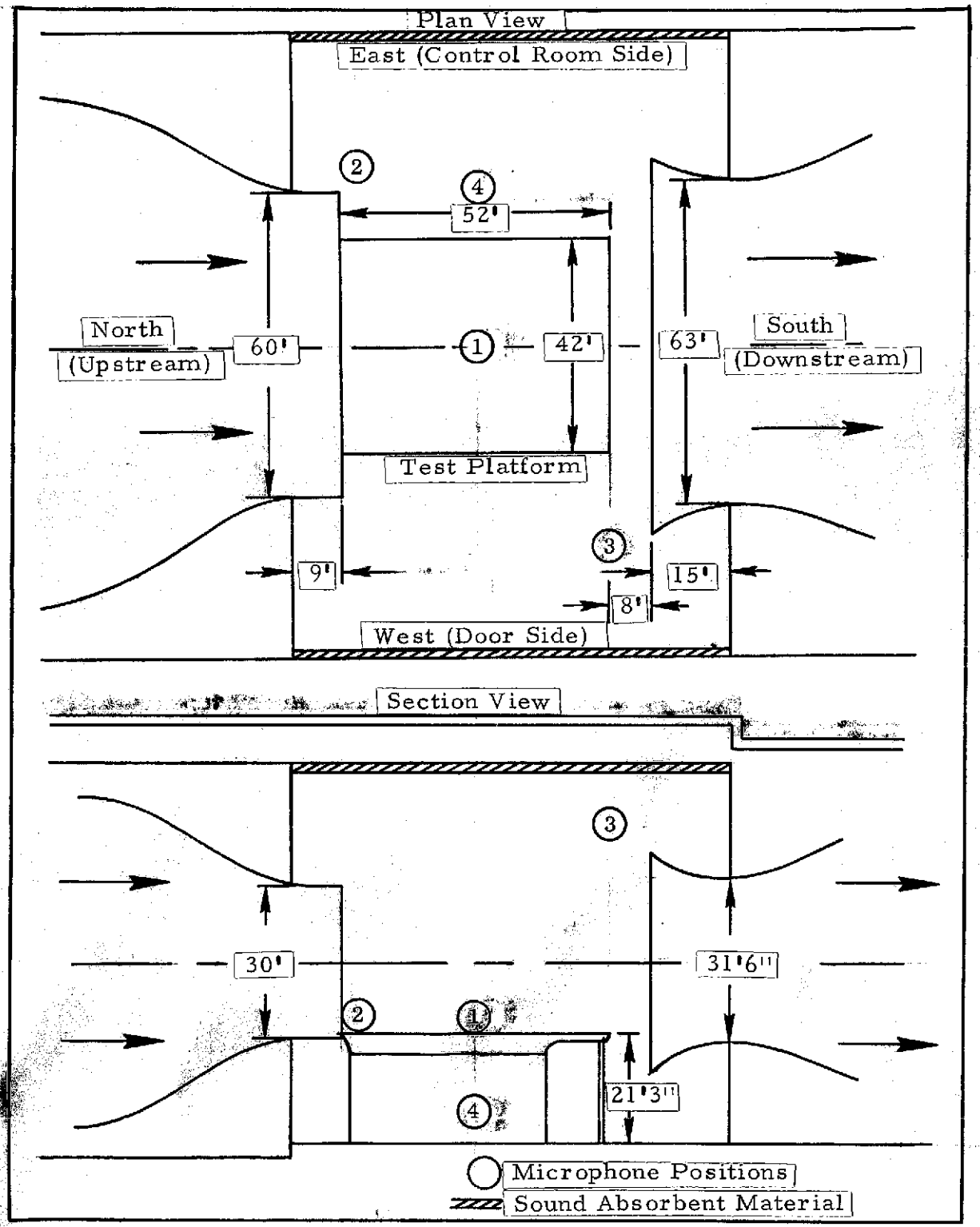

Figure 1. Plan and Elevation Views of Full-Scale Wind Tunnel Test Section Showing Microphone Positions for Ambient Noise Measurements.

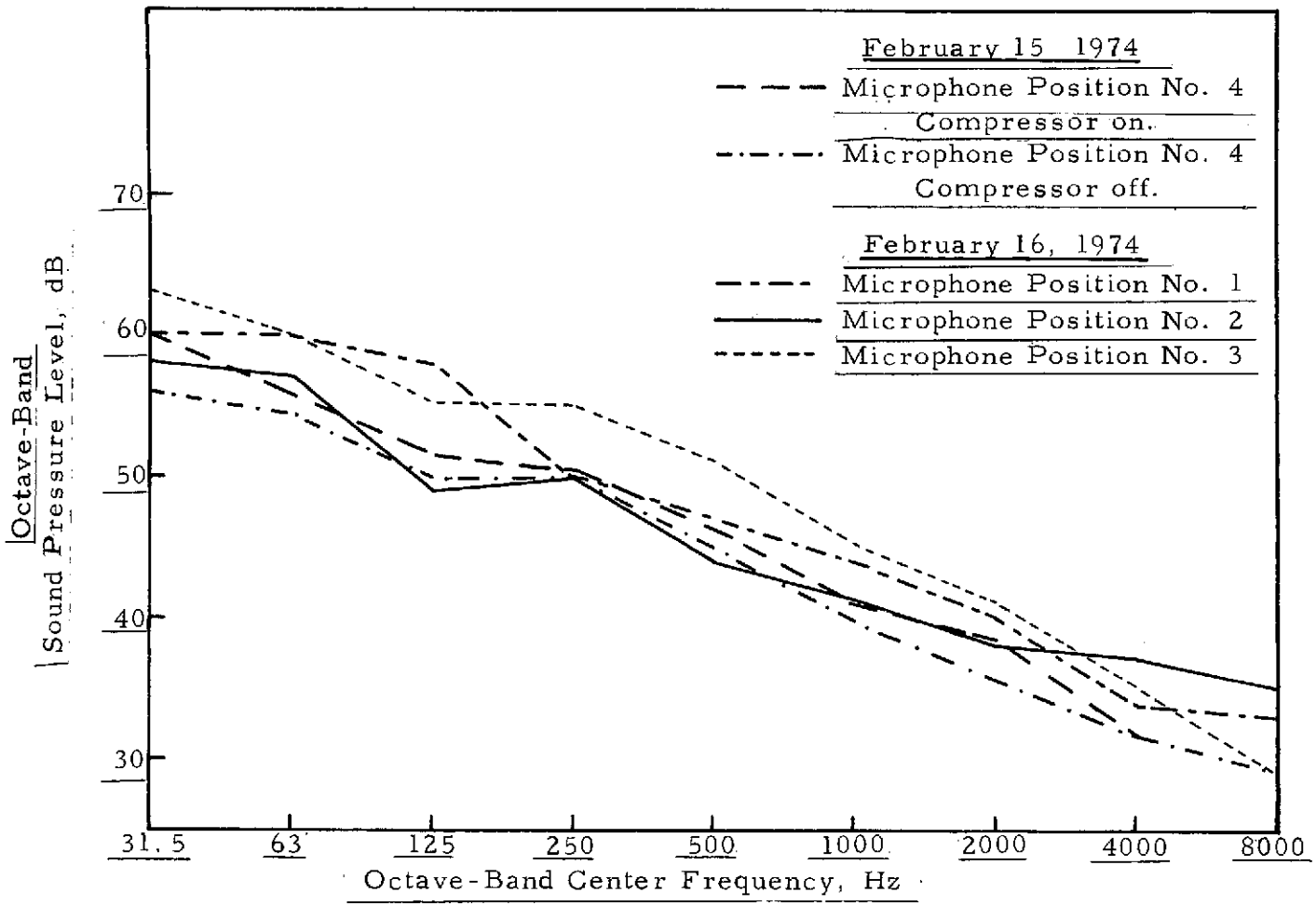

Figure 2. Ambient Noise Level in Test Section.

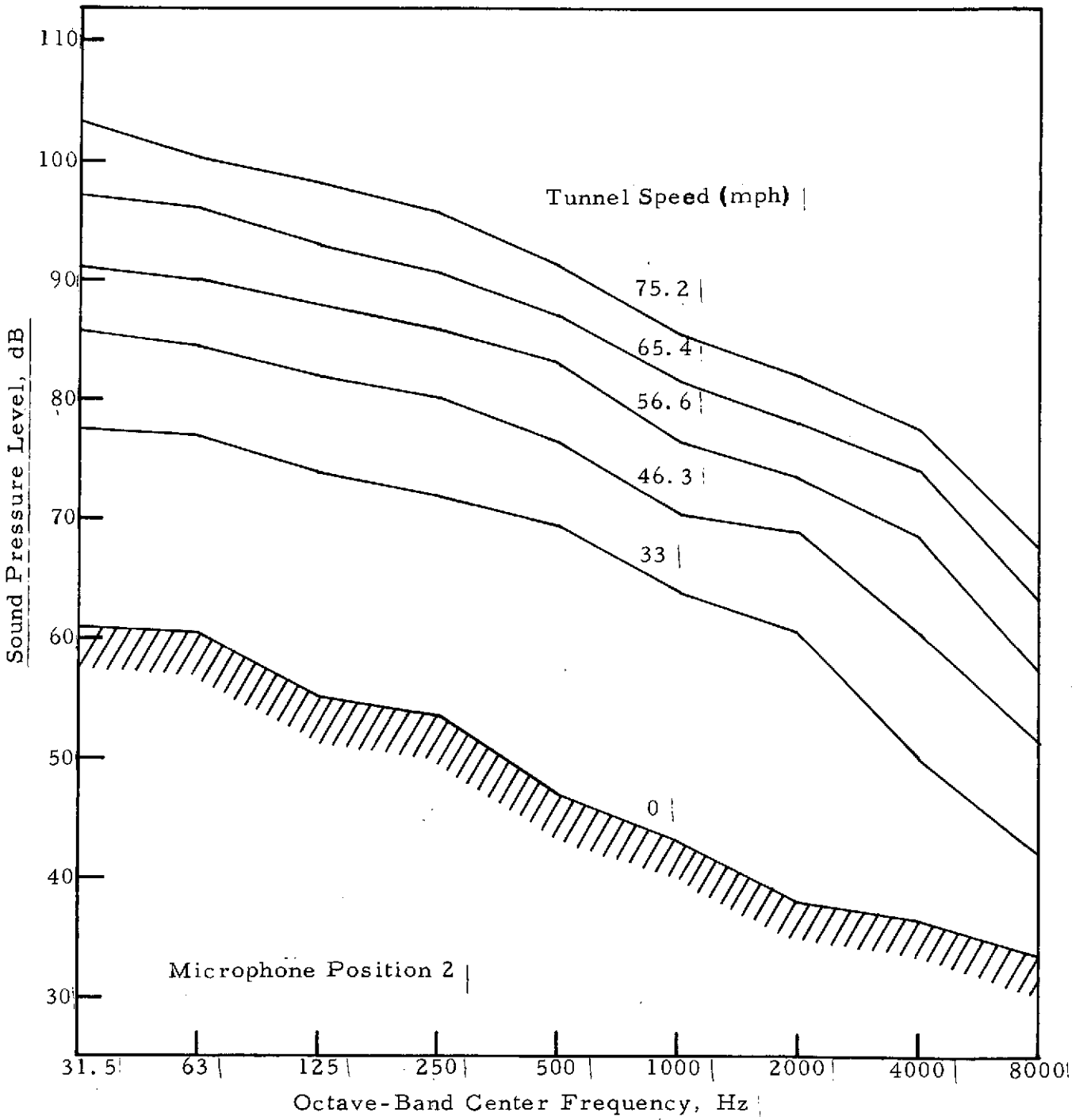

Figure 3a. Octave-Band SPL in Test Section as a Function of Air Speed: Position No. 2.

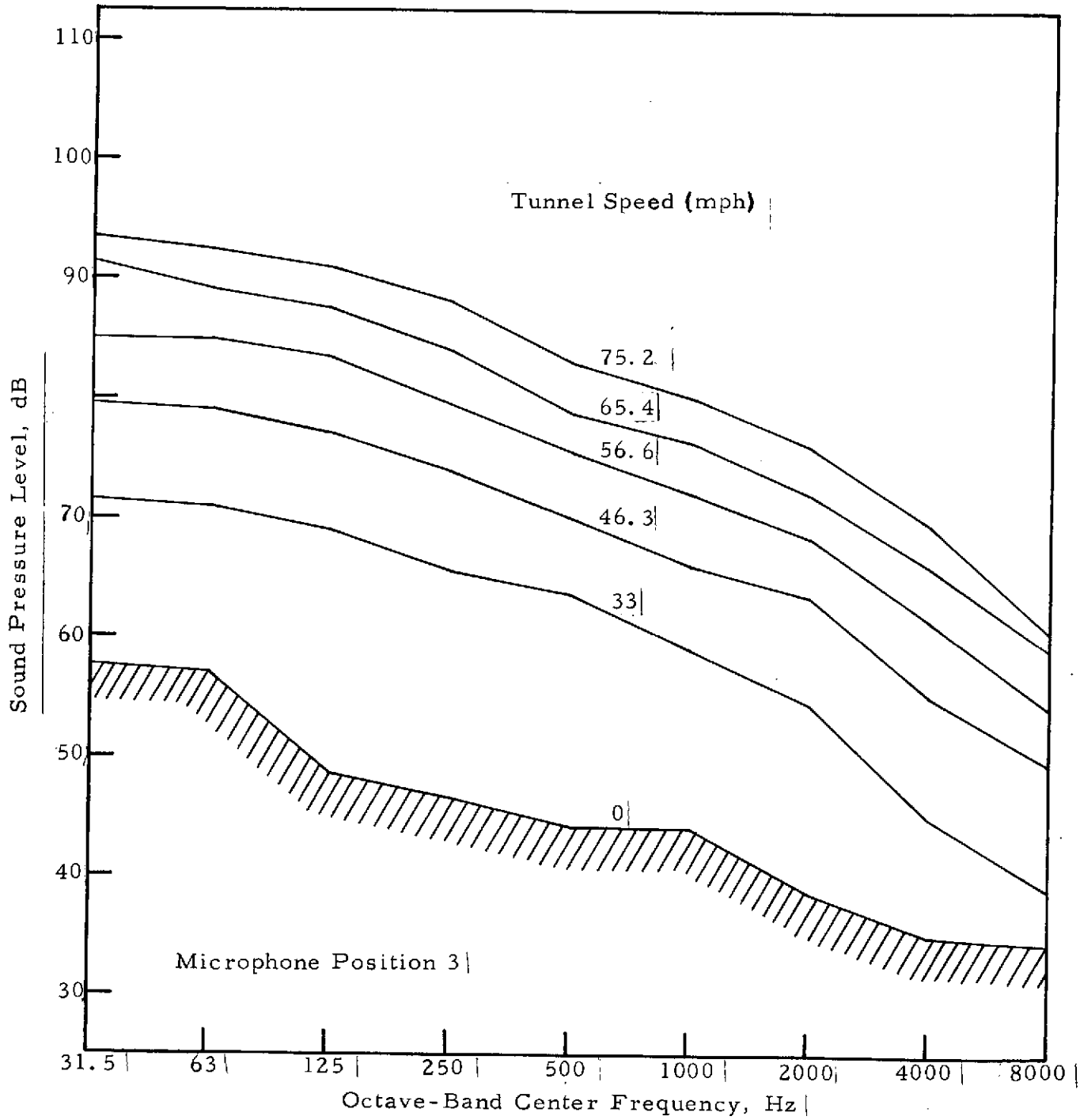

Figure 3b. Octave-Band SPL in Test Section as a Function of Air Speed: Position No. 3.

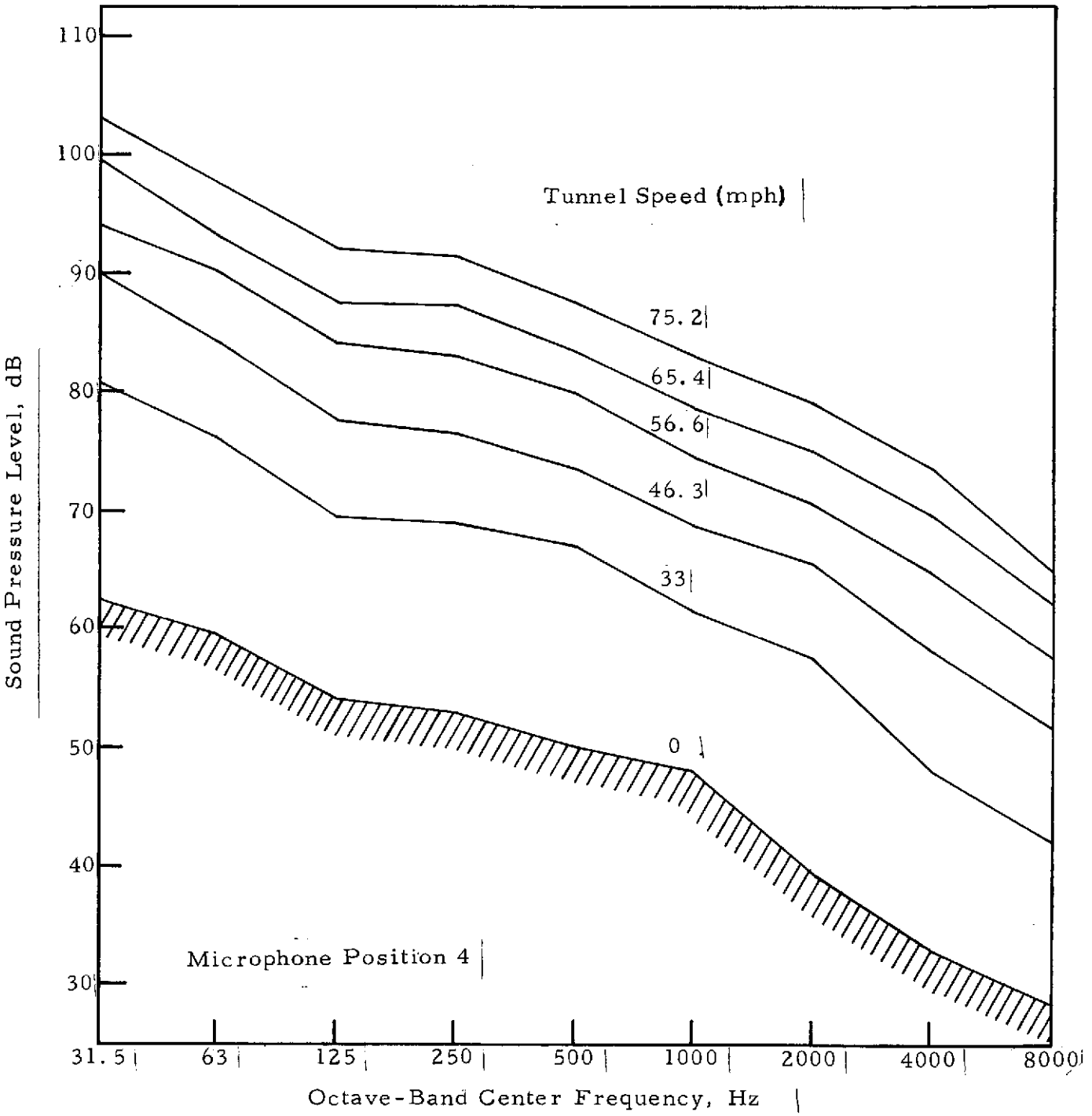

Figure 3c. Octave-Band SPL in Test Section as a Function of Air Speed: Position No. 4.

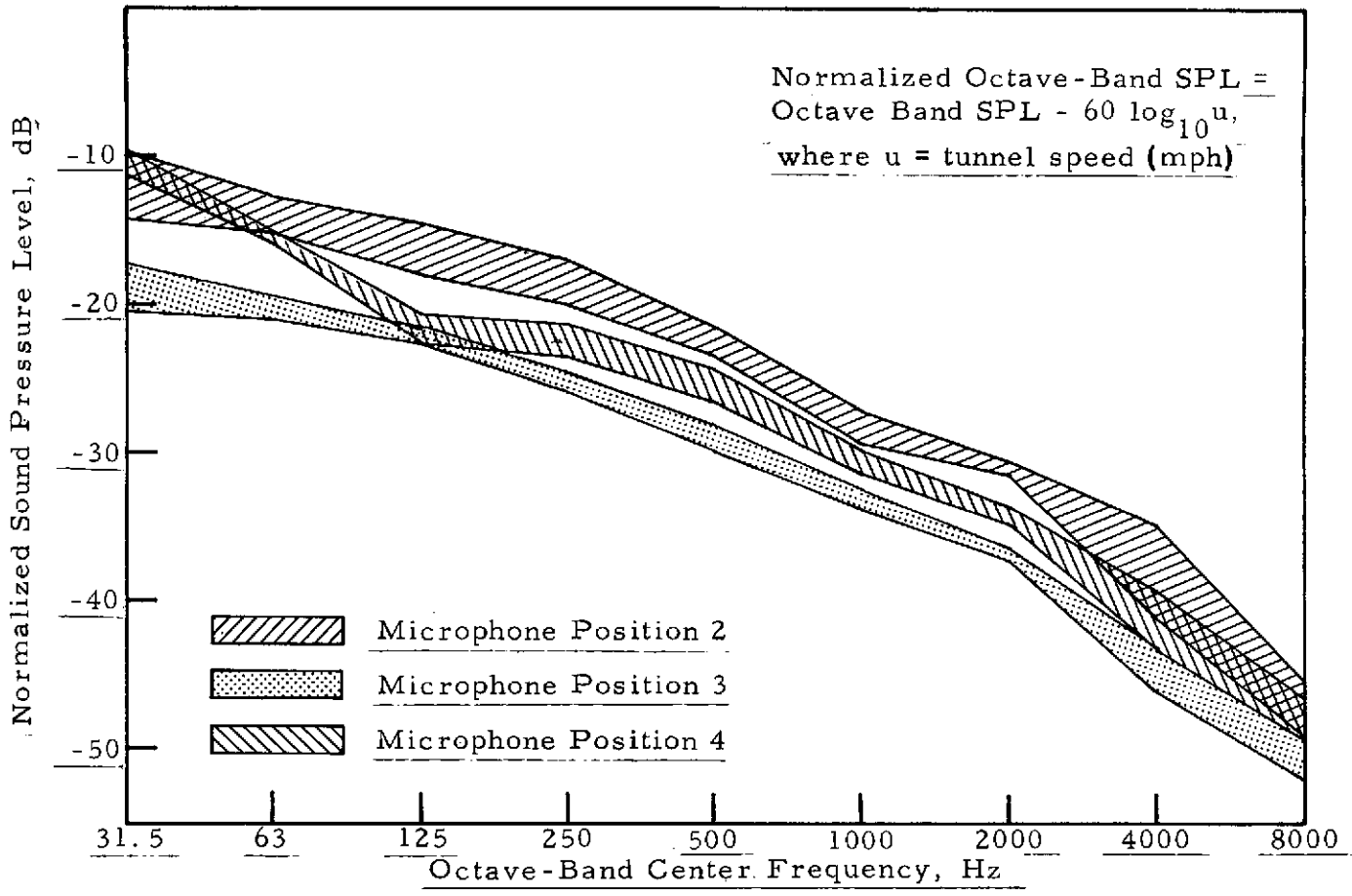

Figure 4. Normalized Octave-Band Ambient Noise Level.

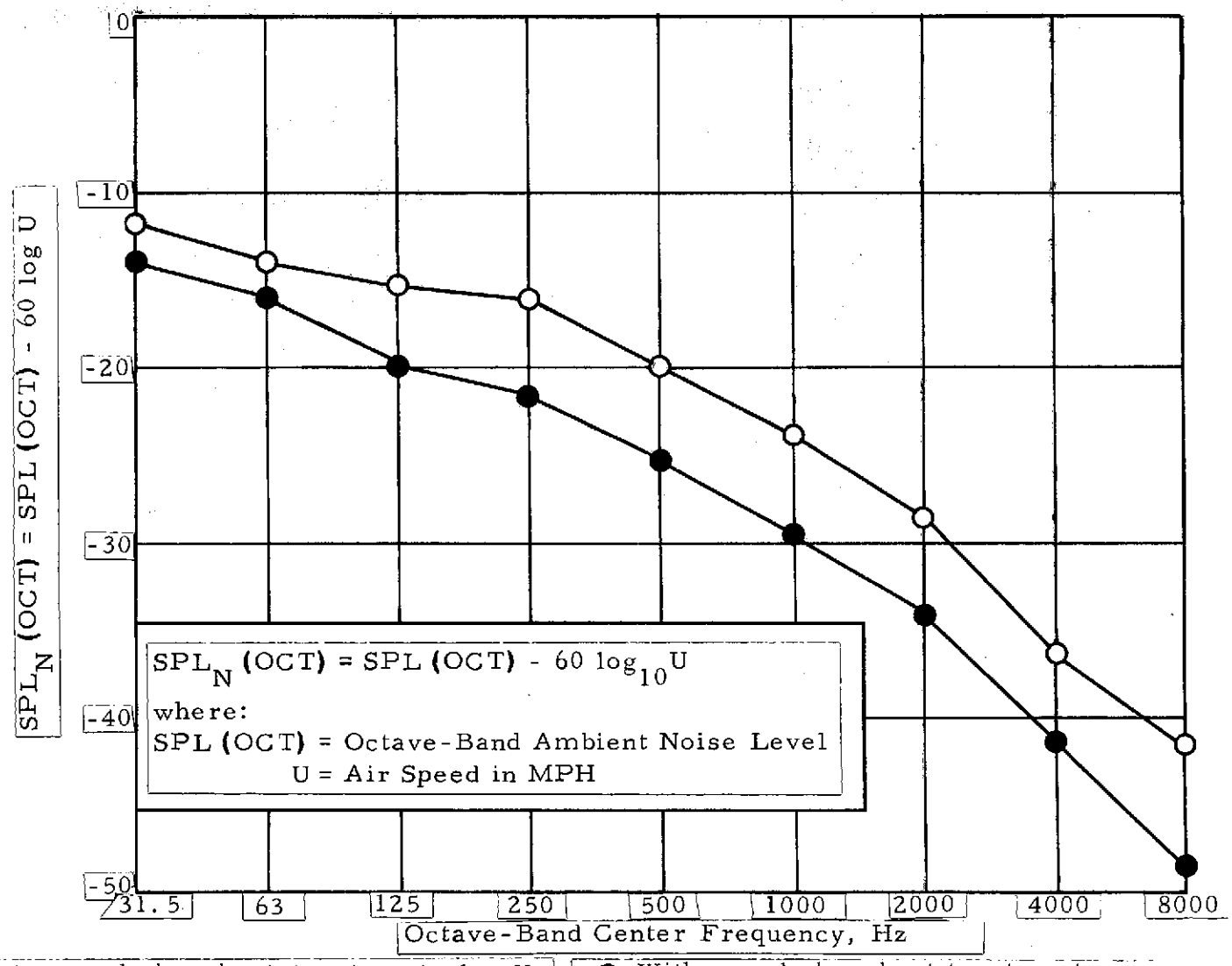

Figure 5. Comparison of Mean Normalized Octave-Band Ambient Noise Measurements Made Prior to and After Sound-Absorbent Treatment of Test Section.

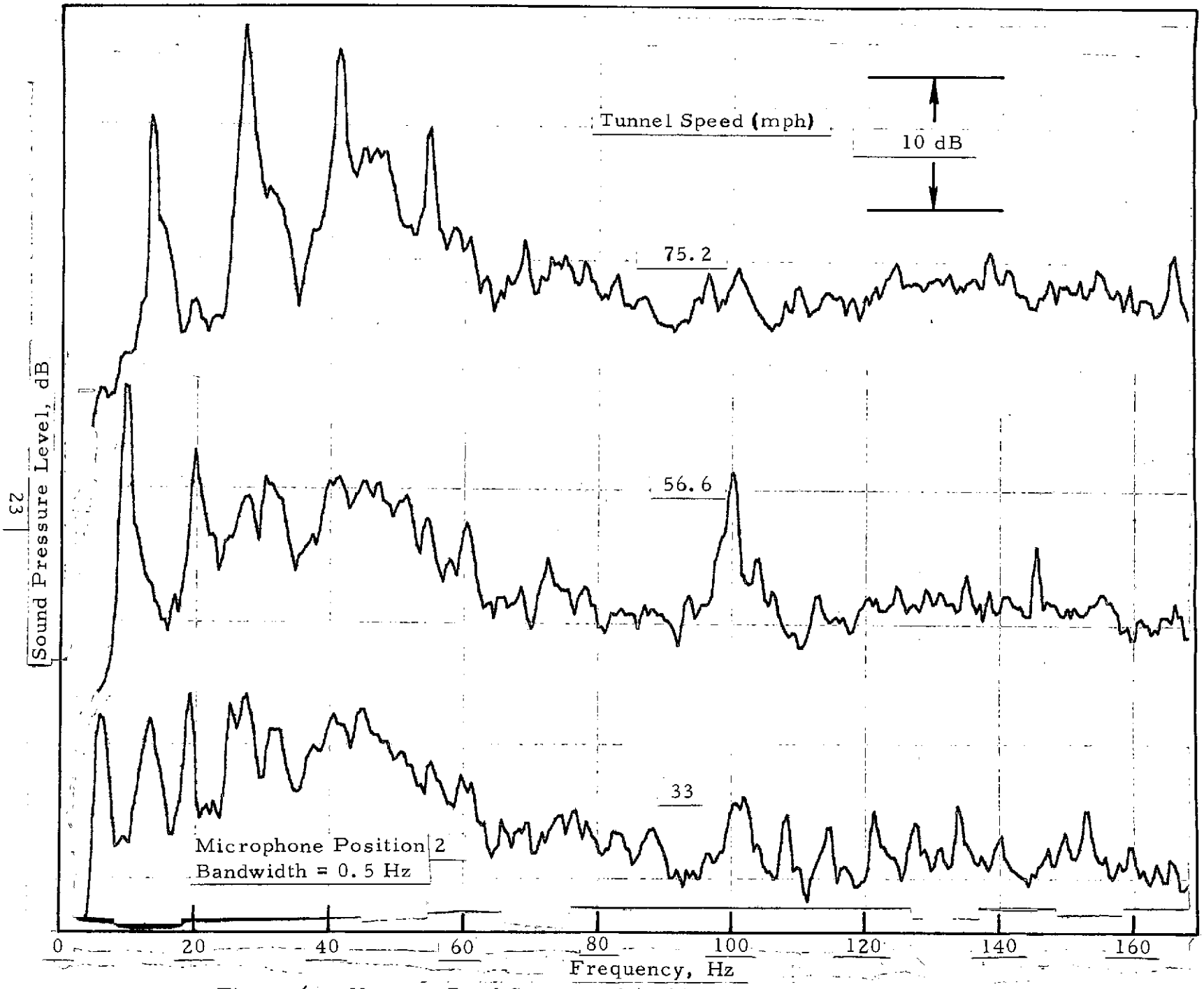

Figure 6. Narrow-Band Spectra of Ambient Level with Tunnel Running, Showing Predominant Rotational Fan Noise Peaks

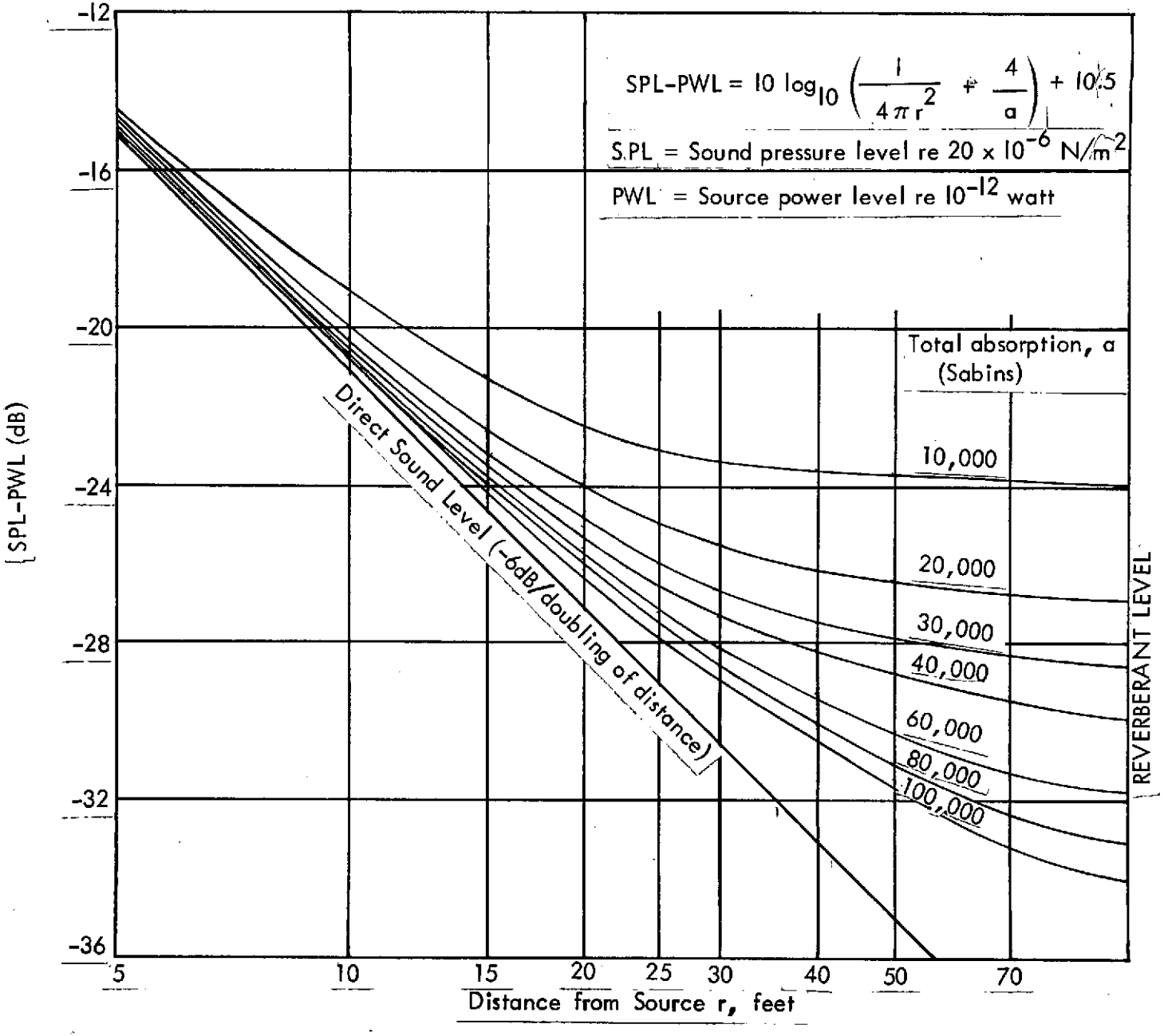

Figure 7. SPL vs. Distance from an Omnidirectional Point Source as a Function of Total Room Absorption, Assuming a Diffuse Reverberant Field.

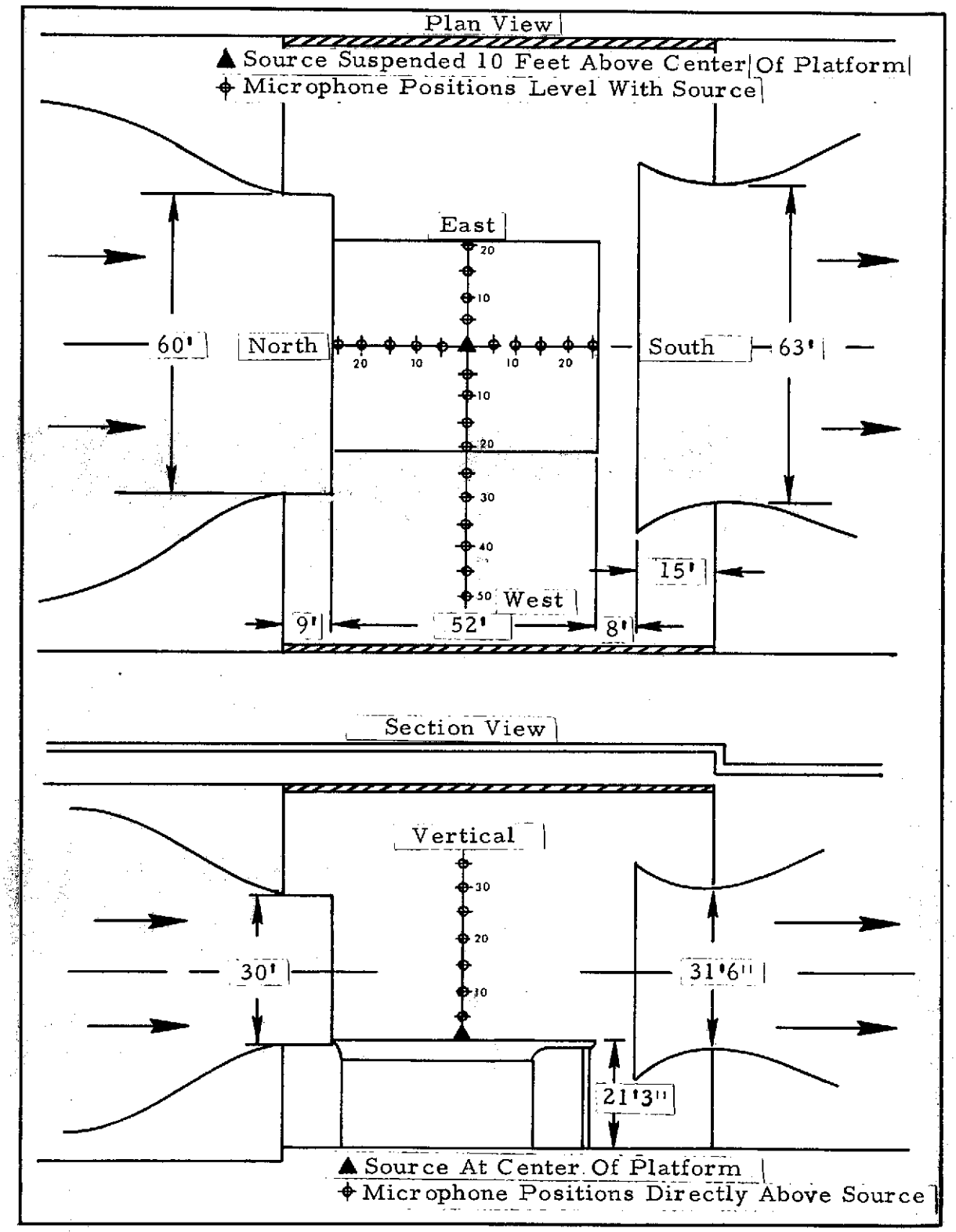

Figure 8. Source and Microphone Positions for Sound Field Measurements.

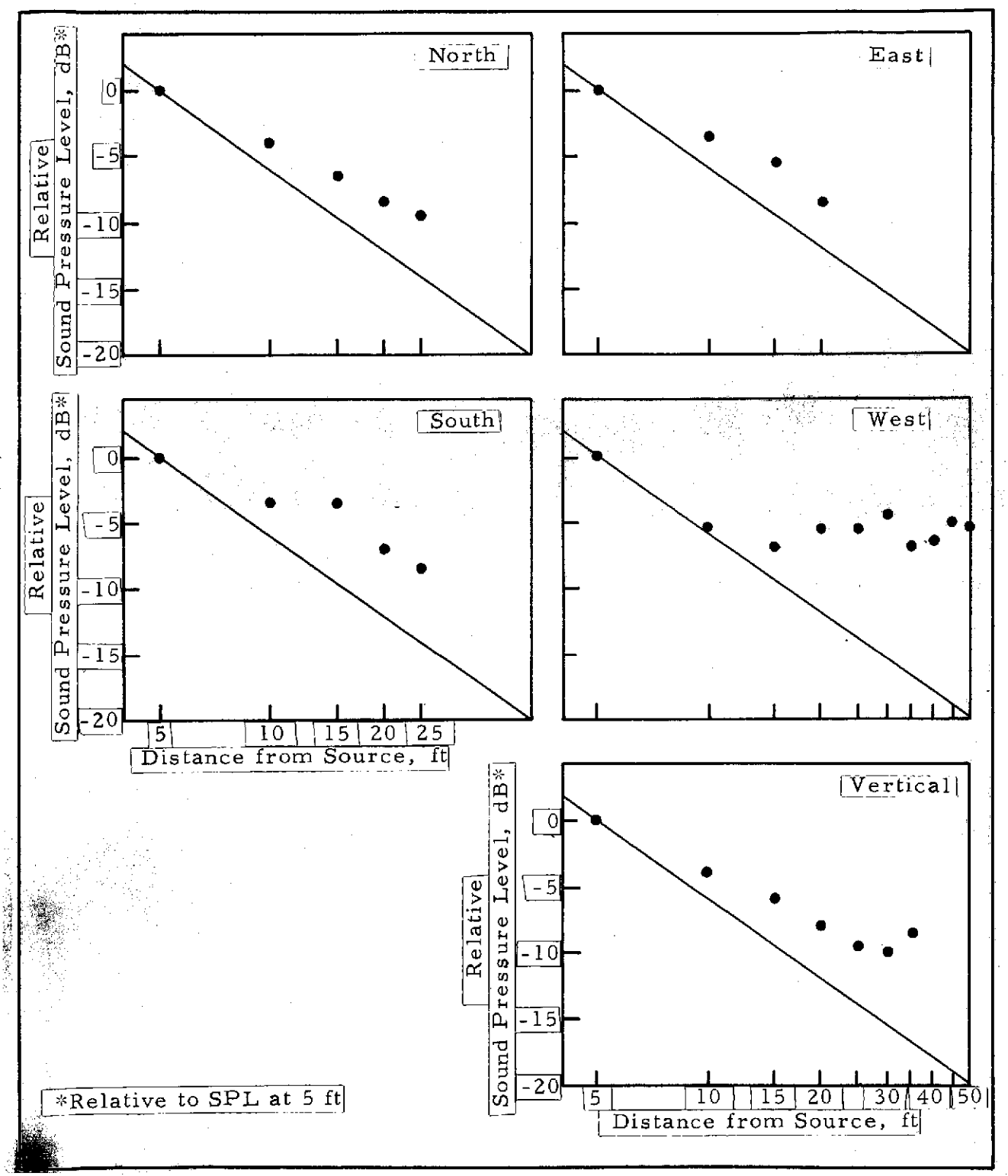

Figure 9a. Measured 63 Hz Octave-Band Sound Pressure Levels in Indicated Directions from Acoustic Source Located at Center of Test Platform.

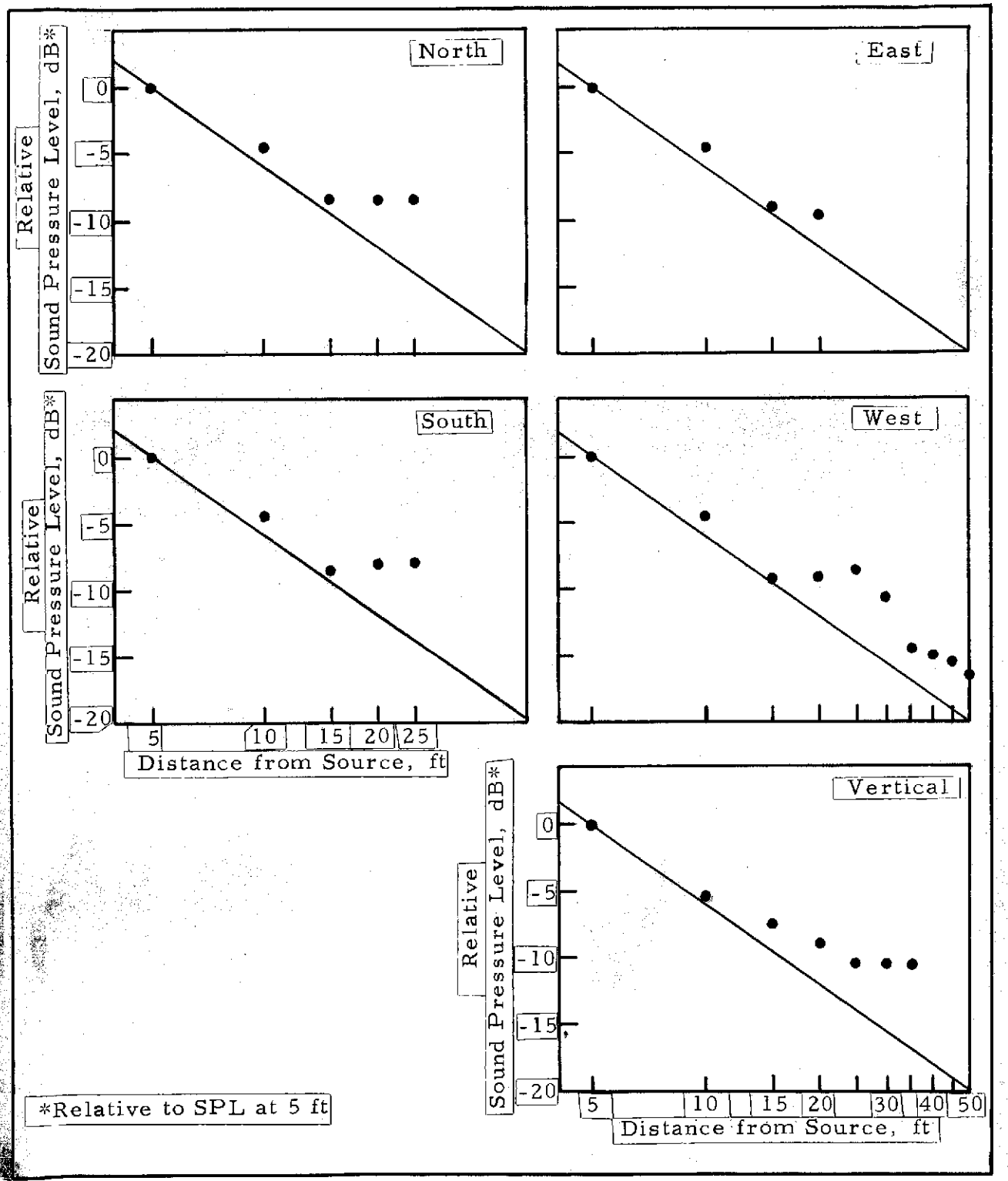

Figure 9b. Measured 125 Hz Octave-Band Sound Pressure Levels in Indicated Directions from Acoustic Source Located at Center of Test Platform.

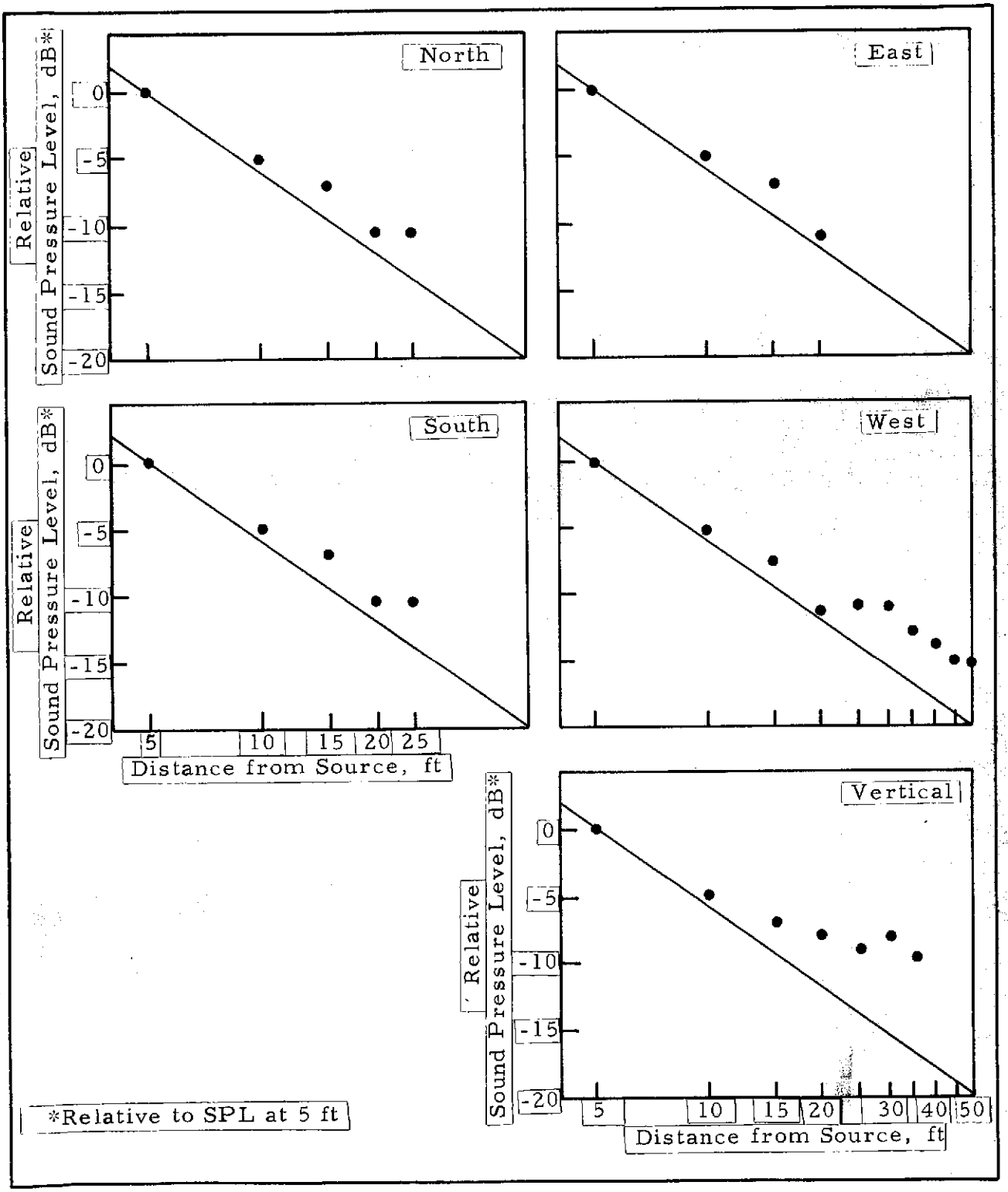

Figure 9c. Measured 250 Hz Octave-Band Sound Pressure Levels in Indicated Directions from Acoustic Source Located at Center of Test Platform.

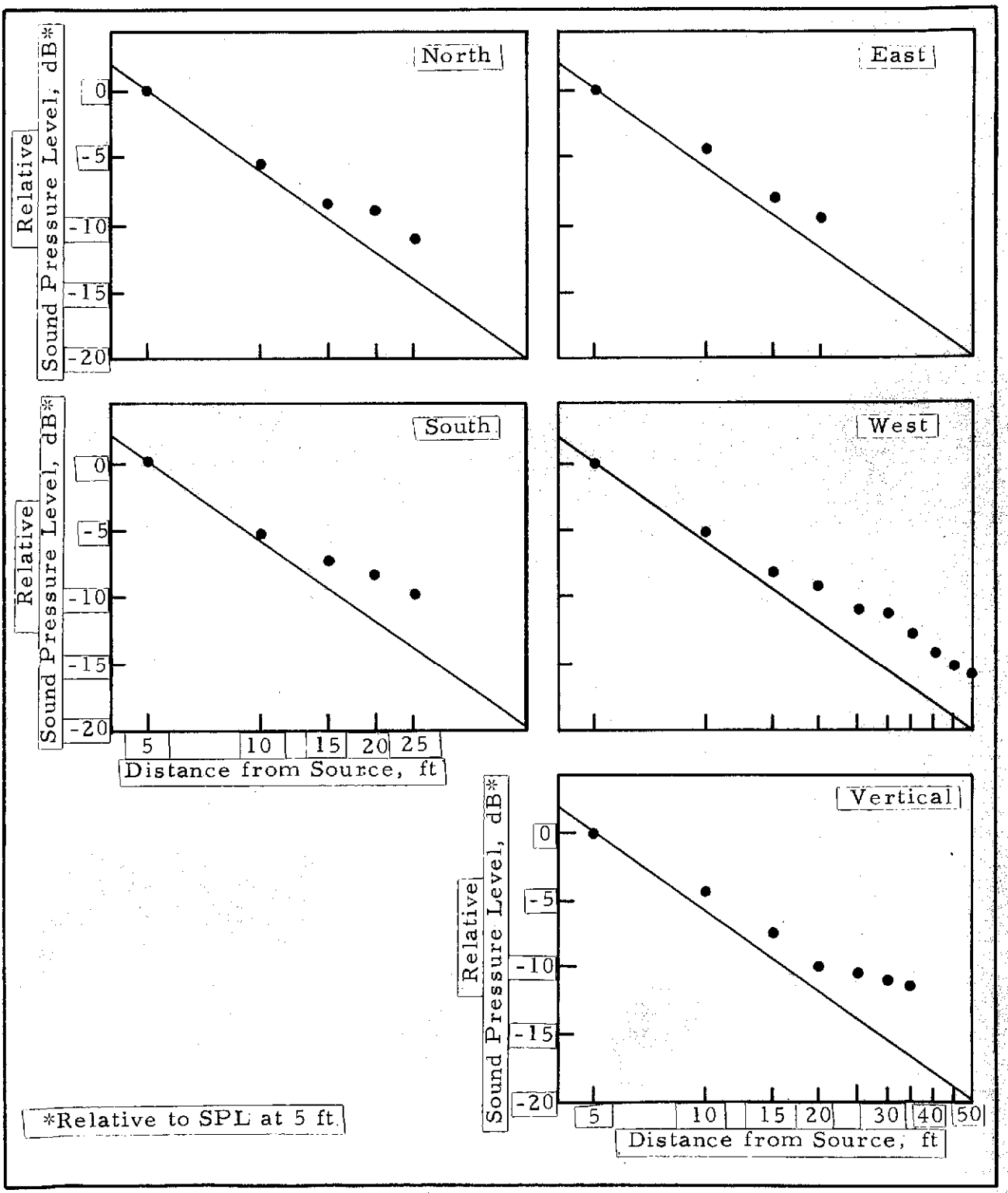

Figure 9d. Measured 500 Hz Octave-Band Sound Pressure Levels in Indicated Directions from Acoustic Source Located at Center of Test Platform.

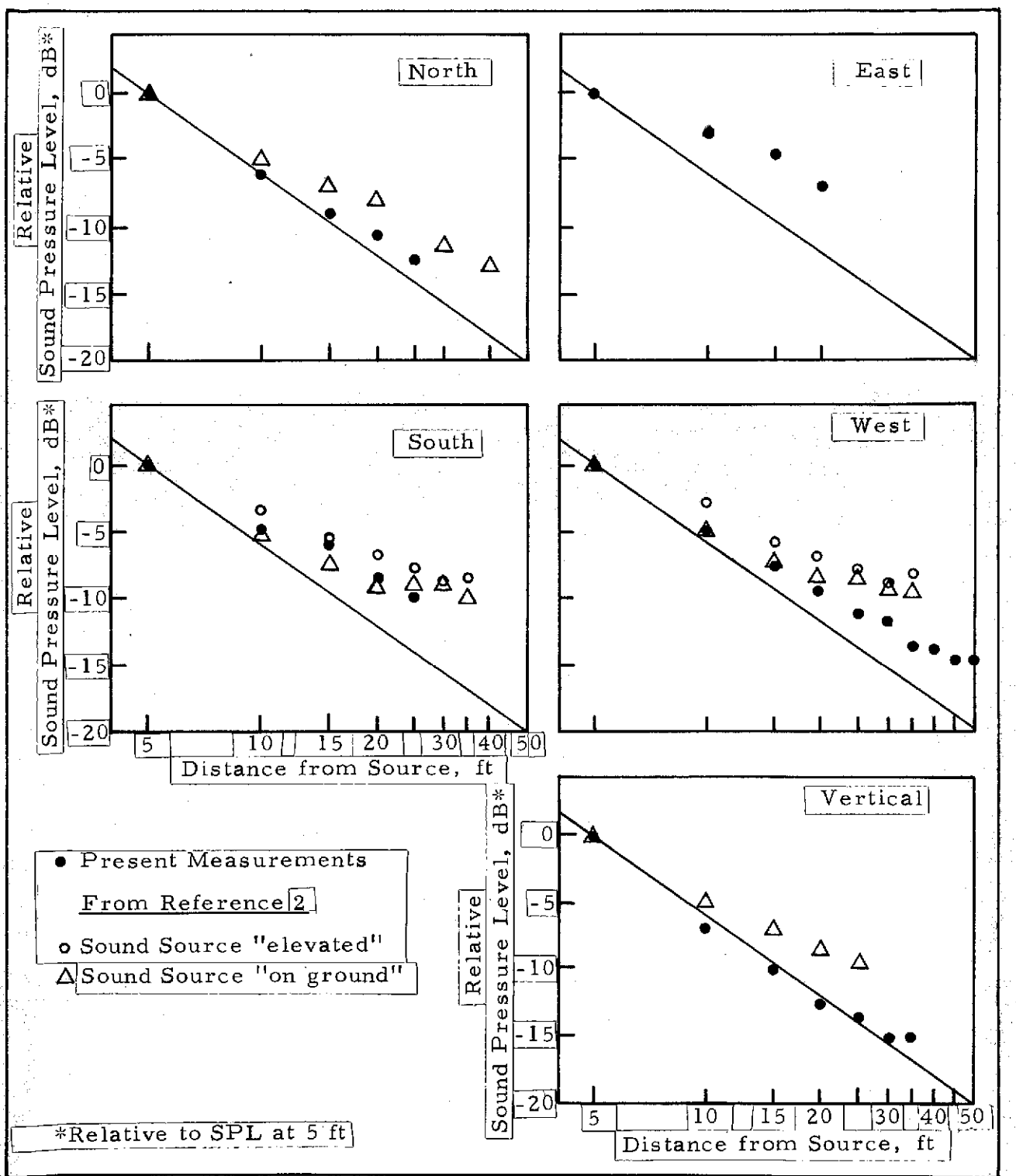

Figure 9e. Measured 1000 Hz Octave-Band Sound Pressure Levels in Indicated Directions from Acoustic Source Located at Center of Test Platform, with Comparison to Previous Measurements.

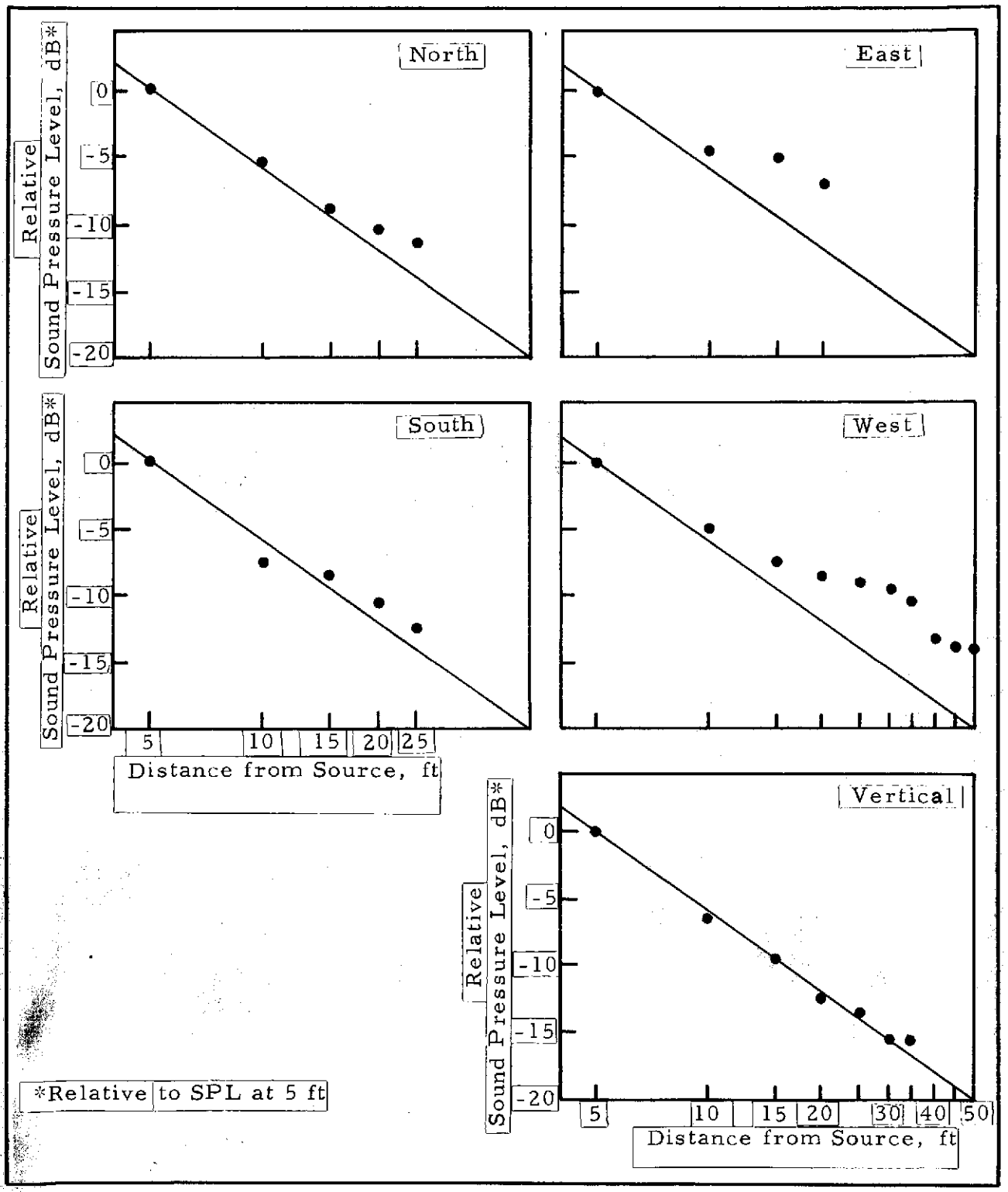

Figure 9f. Measured 2000 Hz Octave-Band Sound Pressure Levels in Indicated Directions from Acoustic Source Located at Center of Test Platform.

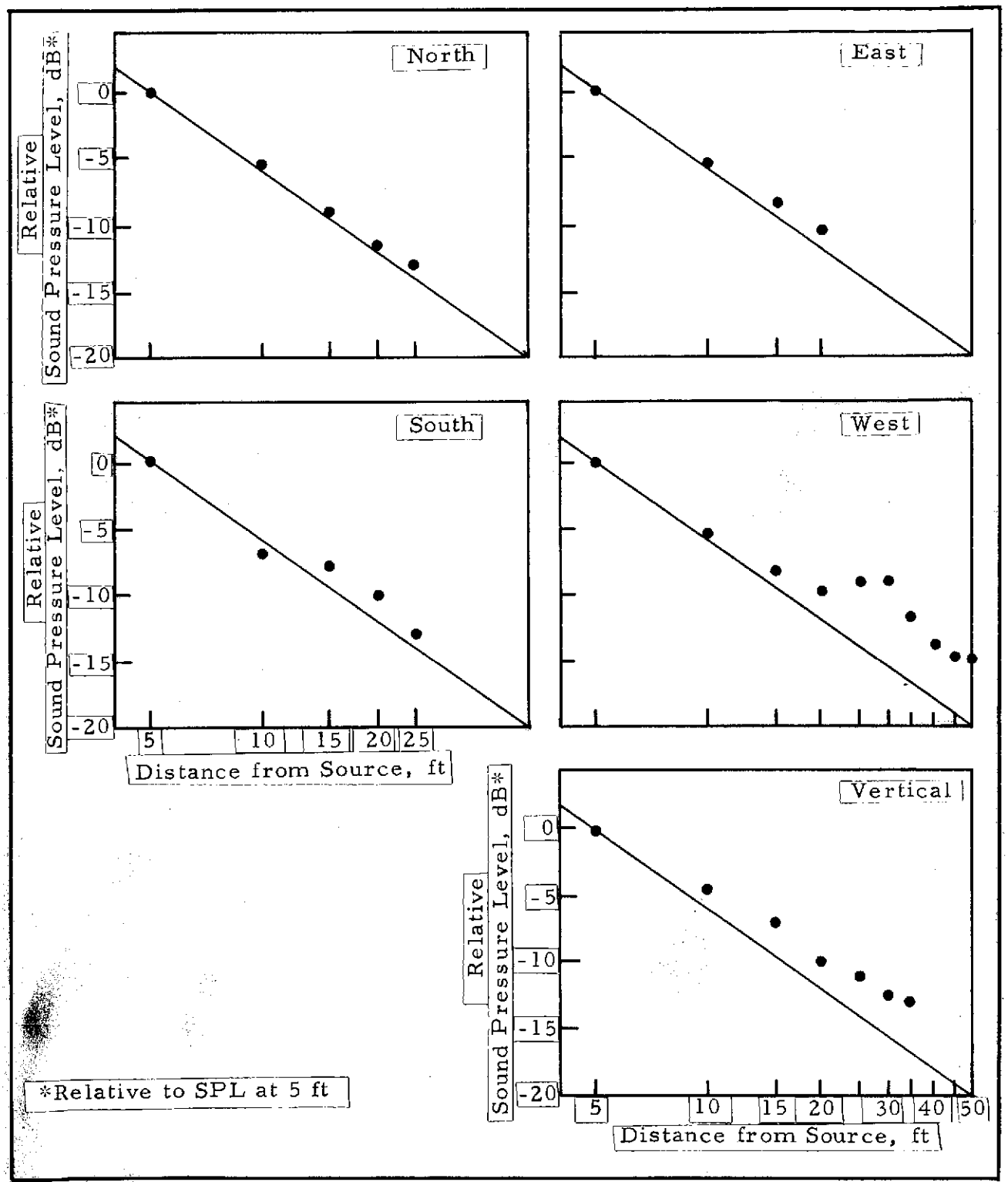

Figure 9g. Measured 4000 Hz Octave-Band Sound Pressure Levels in Indicated Directions from Acoustic Source Located at Center of Test Platform.

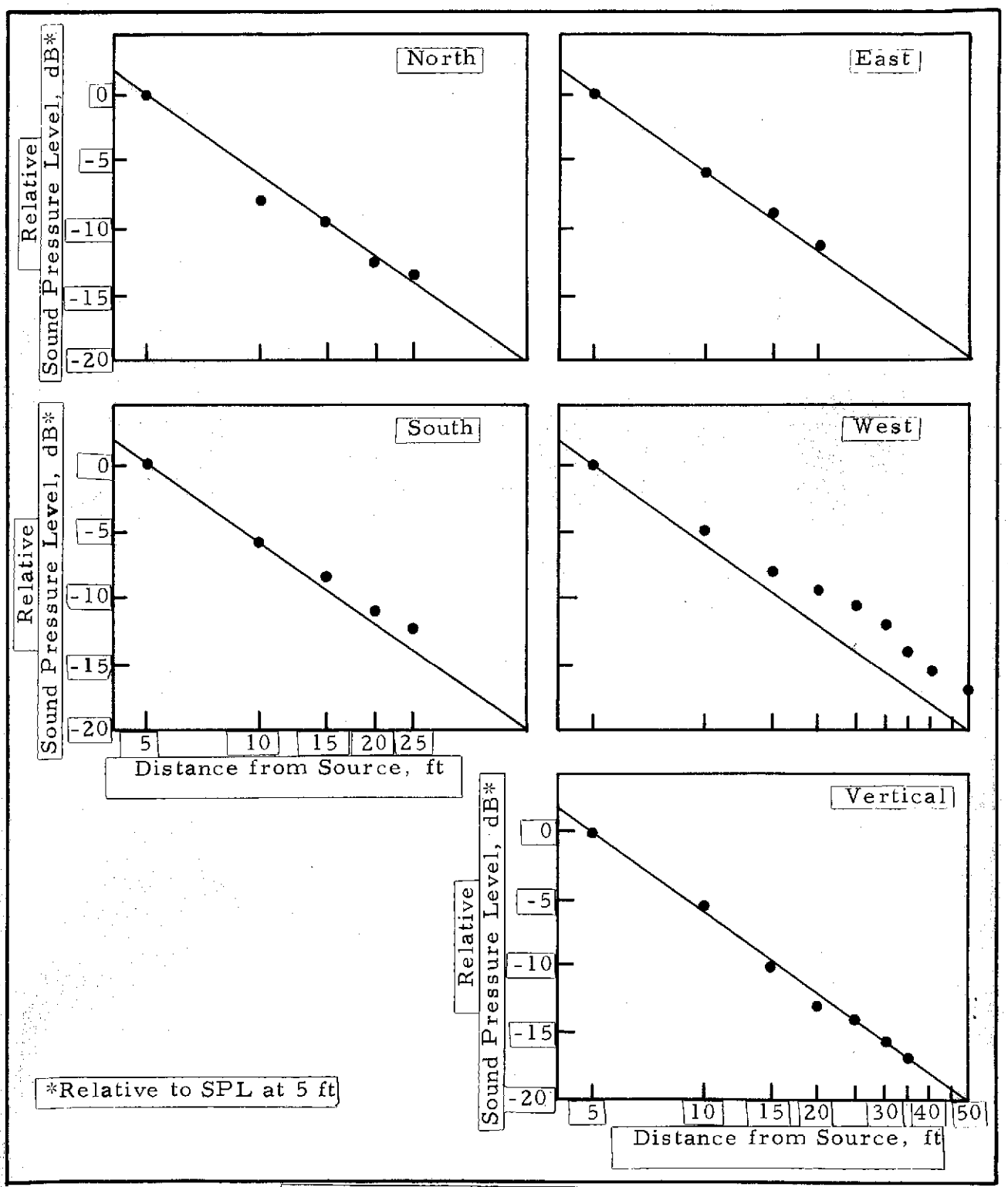

Figure 9h. Measured 8000 Hz Octave-Band Sound Pressure Levels in Indicated Directions from Acoustic Source Located at Center of Test Platform.

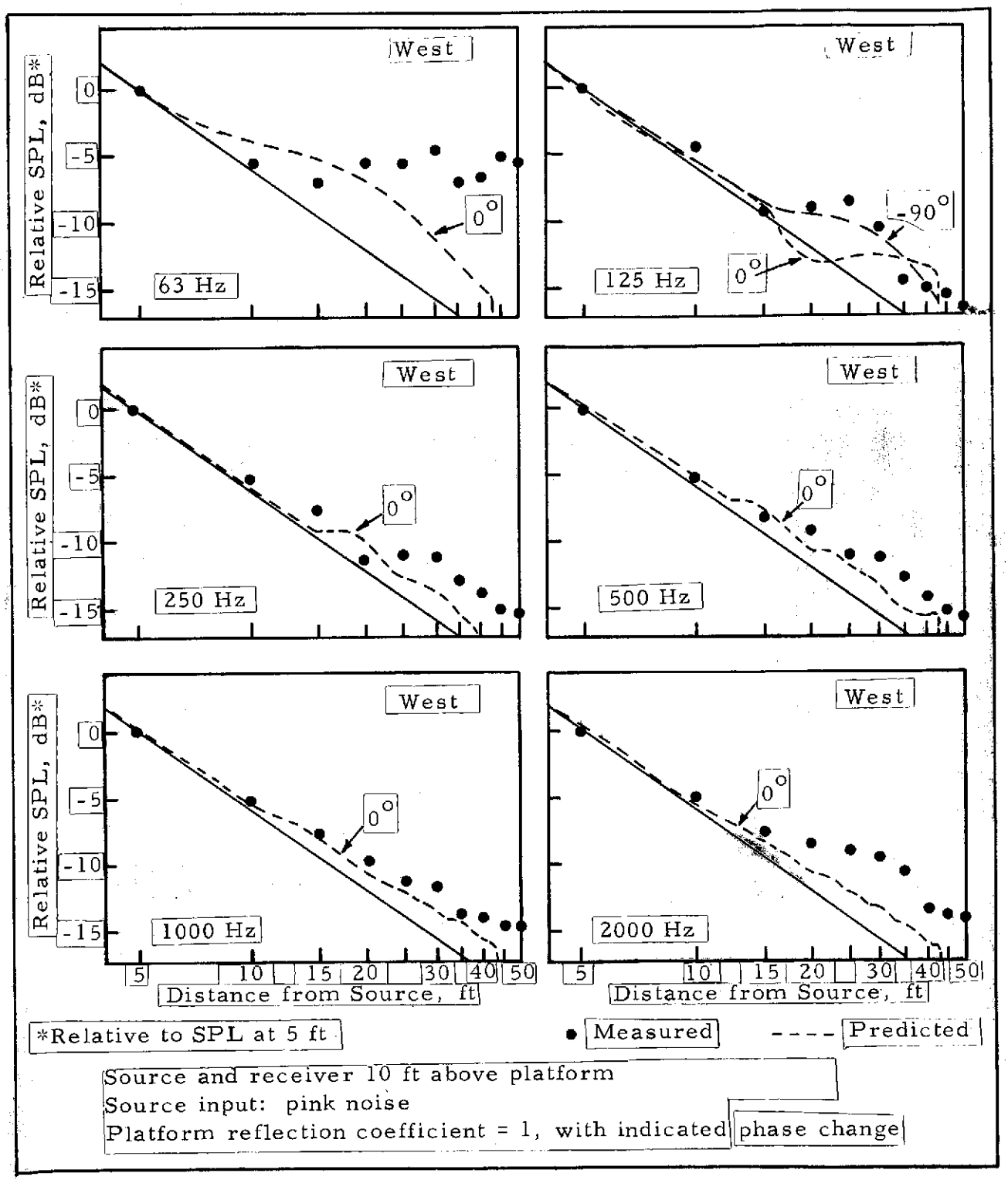

Figure 10. Comparison of Measured Octave-Band Sound Levels with Theoretical Values Considering the Effect of Platform-Reflected Sound, as a Function of Distance from Acoustic Source.

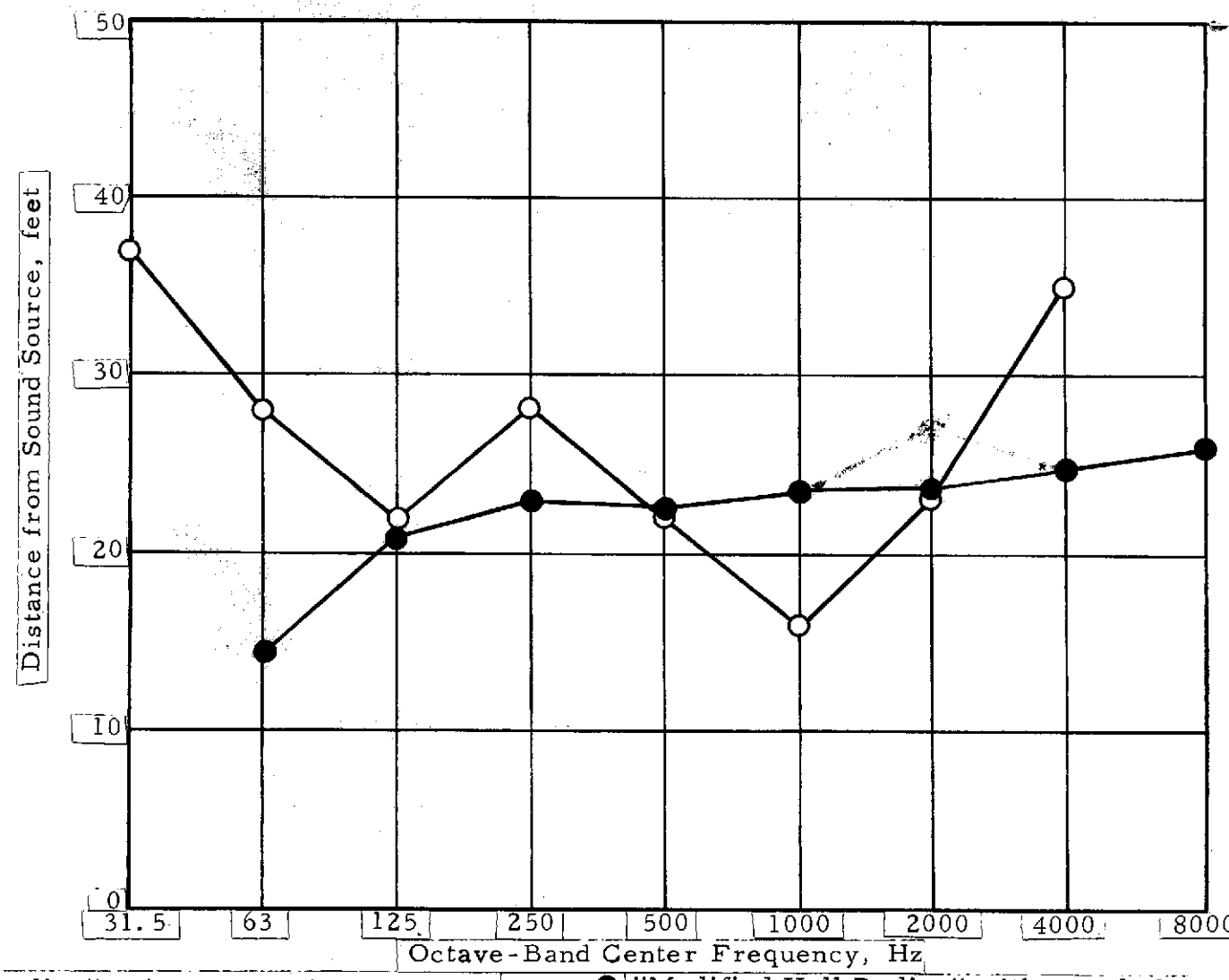

○ "Hall Radius" prior to sound-absorbent treatment of walls and ceiling of test section (Reference 2).

● "Modified Hall Radius" with sound-absorbent treatment. (Determined graphically from Octave-Band SPL vs. Distance curves.)

Figure 11. Comparison of Average Octave-Band "Modified Hall Radius" Distances with "Hall Radius" Values Measured Prior to Sound-Absorbent Treatment of Test Section.

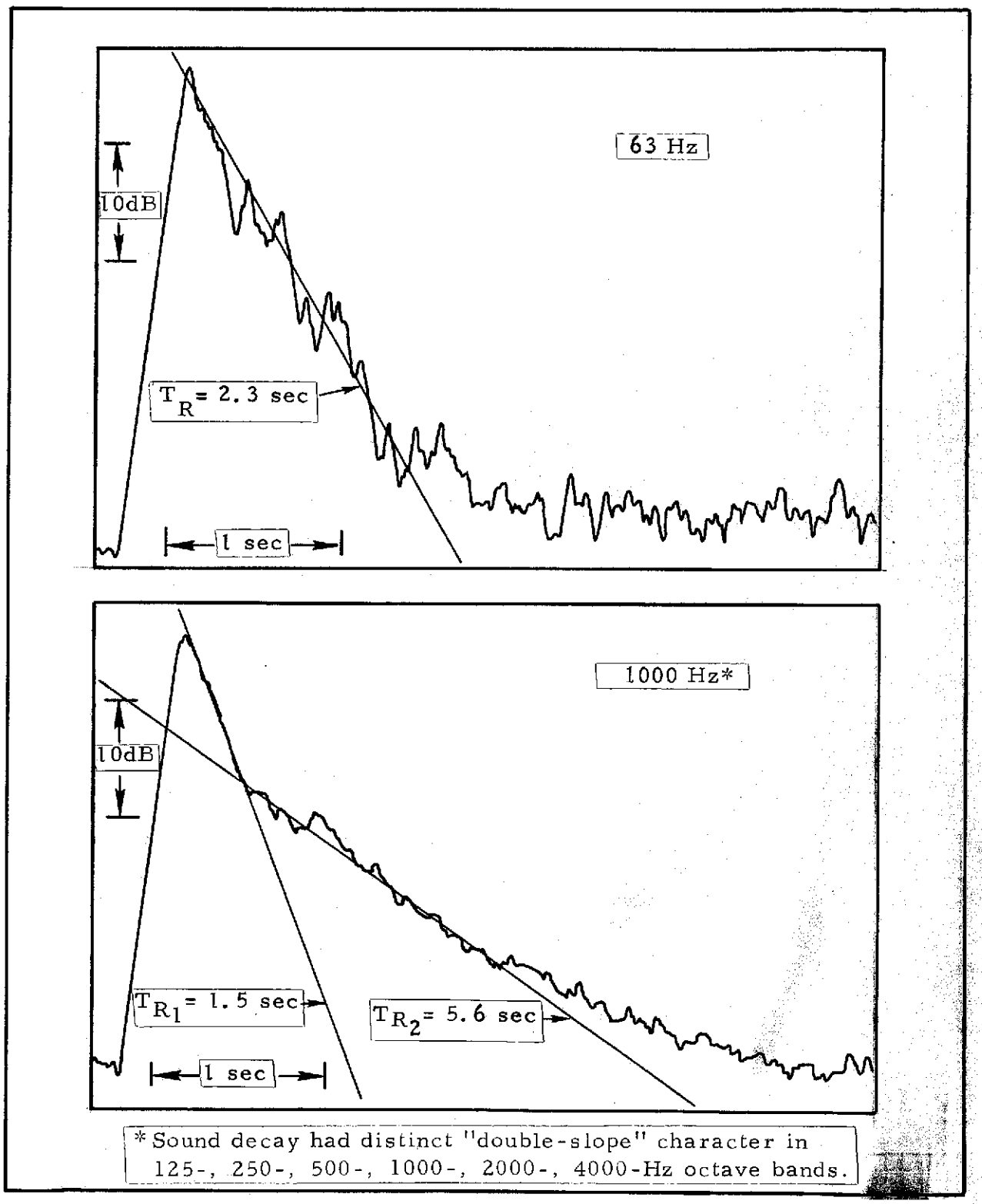

Figure 12. Typical Octave-Band Sound Decay Curves, Showing Measured Reverberation Times.

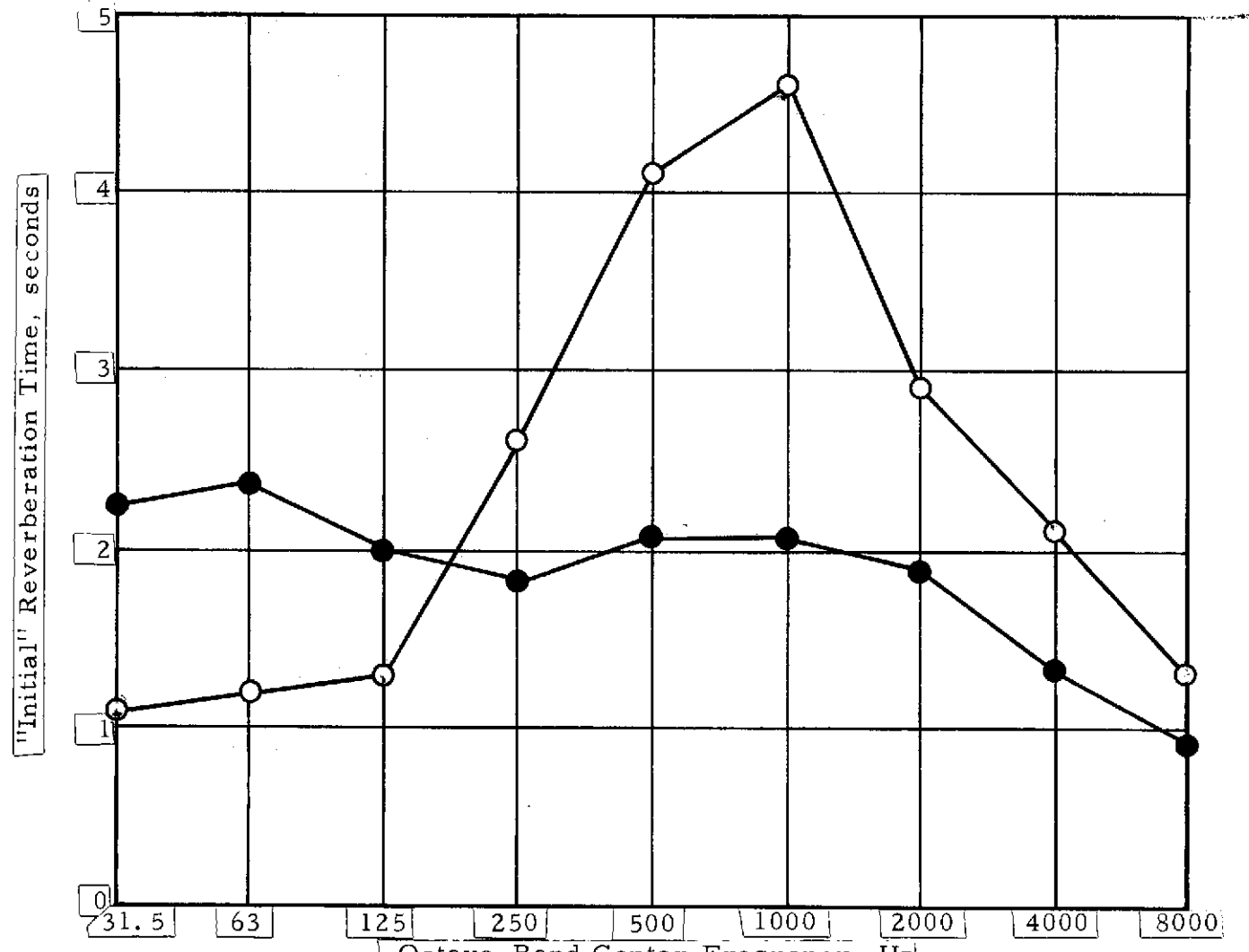

Figure 13. Comparison of Average Octave-Band Reverberation Times with Measurements Made Prior to Sound-Absorbent Treatment of Test Section.

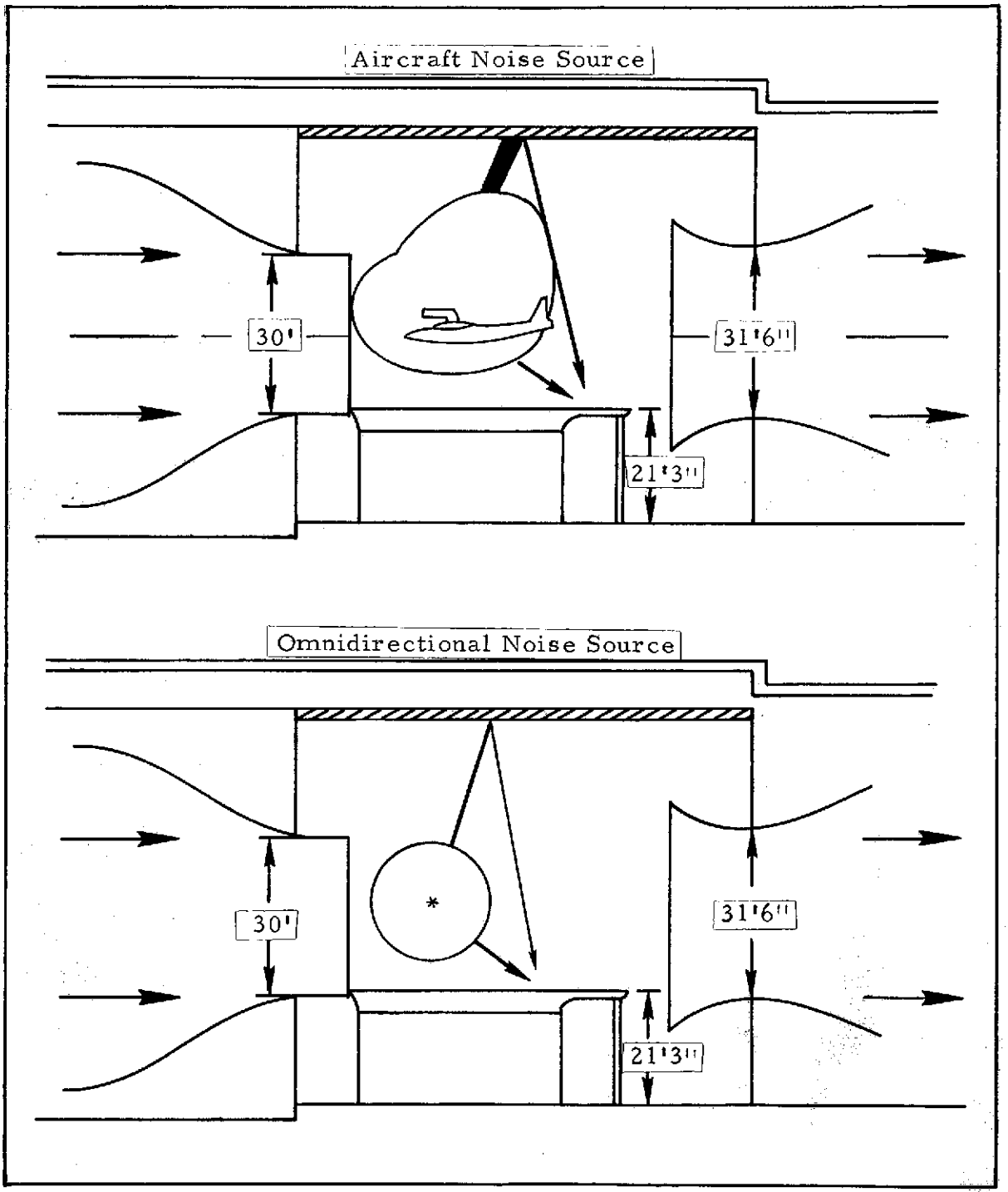

Figure 14. Effect of Reflected Component Magnitudes on Measured Sound Pressure Levels Due to Sources with Differing Directional Characteristics.